LBL-30574

AIR MOVEMENT, COMFORT AND VENTILATION IN WORKSTATIONS

F.S. Bauman*, D. Faulkner+, E.A. Arens*, W.J. Fisk+,
L.P. Johnston*, P.J. McNeel+, D. Pih+, and H. Zhang*

*Center for Environmental Design Research
University of California at Berkeley
Berkeley, CA 94720

+Indoor Environment Program
Applied Science Division
Lawrence Berkeley Laboratory
Berkeley, CA 94720

April 1991

This work was supported by Steelcase, Inc. and by the Assistant Secretary for Conservation and Renewable Energy, Office of Building Technologies, Building Systems and Materials Division of the U.S. Department of Energy (DOE) under Contract No. DE-AC03-76SF00098.

AIR MOVEMENT, COMFORT, AND VENTILATION IN WORKSTATIONS

Final Report
April 1, 1991

ABSTRACT

This report presents findings from a research project to investigate the effects of office partition design on air movement, worker comfort, and ventilation in workstations. The objectives of the study were to evaluate the comfort and ventilation conditions produced by a conventional ceiling supply-and-return air distribution system in workstations separated by (1) solid partitions of different height (75 in. [1.9 m], 65 in. [1.65 m], 42 in. [1.1 m], and 0 in. [partitions removed]), and (2) prototype Steelcase "airflow" partitions, containing a gap positioned at the bottom of the partition. The project consisted primarily of experiments performed in a full-scale Controlled Environment Chamber (CEC) located in the Building Science Laboratory, Department of Architecture, University of California, Berkeley.

The tests were performed by setting up a typical modular office environment in the CEC using Steelcase Modular Workstations. The range of partition configurations and environmental parameters investigated included: (1) partition height, (2) solid vs. airflow partitions, (3) airflow gap size, (4) supply air volume, (5) supply/room temperature difference, (6) supply diffuser location, (7) heat load density, (8) workstation size, and (9) cooling vs. heating mode. Under steady-state conditions, multipoint measurements were made of: (1) thermal environment -- measurements of air velocities and temperatures along with radiant (globe) temperatures to characterize the key environmental variables affecting thermal comfort; and (2) ventilation efficiency -- tracer gas methods were used to determine the ventilation performance within the test chamber.

The test results were analyzed and compared to evaluate the relative performance of each test configuration. Data analysis was performed using the following methods: (1) the ASHRAE Air Diffusion Performance Index (ADPI) method [1] was used to quantify overall air diffusion performance; (2) the Fobelets and Gagge two-node comfort model

[2] was used to predict characteristic comfort indices at typical work locations within each workstation; (3) thermal acceptability was determined in accordance with ASHRAE Standard 55-81 [3]; and (4) the age-of-air method was used to evaluate the spatial variability of ventilation.

The results indicate that variations in solid partition height produce only small differences in overall thermal and ventilation performance. Results also show that while the existence of an airflow opening at the bottom of office partitions can, in some cases, produce slight increases in air velocities near the floor, there are no significant improvements in comfort conditions or ventilation efficiency within the workstations compared to results obtained for solid partitions. Test parameters that were found to have a more substantial impact on air movement and comfort included heat load density and distribution, supply air temperature, and supply diffuser location. Deviations from uniform workstation ventilation were small during all cooling mode tests. Some short-circuiting of the supply air to the return air occurred during heating mode tests.

INTRODUCTION

Recent developments in office design, function, and technology make it increasingly difficult for conventional centralized HVAC systems to satisfy the environmental preferences of individual office workers. Valuable data from several recent large office building occupant surveys more precisely define the range of environmental factors that are critically related to the interdependent relationships between a building and its occupants [4-9]. In today's typical open plan office building, the design and layout of workstation furniture and partitions can play an important role in determining the nature of many of these environmental factors, including thermal and airflow conditions, noise and spatial privacy, and the functionality of the workplace. Workstations are frequently separated by partitions that may, under certain conditions, divert the flow of air between conventional, ceiling-mounted supply diffusers and return registers so that the workstations themselves are not well ventilated. The workstations are also often reconfigured to accommodate changing tenant needs, affecting the HVAC system's ability to meet the loads for which they were designed. Modern offices also have large amounts of heat-generating equipment (computers, printers, etc.) whose loads may vary

considerably from workstation to workstation. Finally, with the growing awareness of the importance of the comfort, health, and productivity of office workers, the increased demand among employers and employees for a high-quality work environment cannot always be met by conventional HVAC and office design approaches.

Standards for maintaining comfortable indoor thermal environments have been developed by ASHRAE [3] and ISO [10]. Both of these standards specify a zone of relatively uniform conditions within which no more than 20% of the occupants are expected to be dissatisfied. Although 20% is in itself a fairly large number, a recent field study in office buildings suggests that the dissatisfaction level for environments maintained within the comfort zone may in fact be substantially higher [9]. In addition, this study and others [11,12] have found that lack of air movement is one of the most common complaints in office environments, although the low air movement rates are mandated by the standards.

There is understandably a great deal of concern among the building engineering community over the potentially detrimental effects of office partitions on air movement, comfort, and air quality. "Airflow" partitions, or partitions that have been raised off the floor, thereby providing a gap for additional air movement between adjacent workstations, have been introduced as one possible means for improving airflow conditions. The currently available literature, however, provides only a few reports describing the effects of partitions (both solid and "airflow") on air movement in office environments.

Hart and Int-Hout tested the influence of 1.5 m (5 ft) vertical acoustical screens placed at various locations with respect to continuous linear diffusers in an open plan office [13]. They measured the ASHRAE-defined Air Diffusion Performance Index (ADPI) [1] and found relatively good performance and circulation for all configurations tested. Public Works Canada (PWC) performed air circulation tests in the Harold Hays Building in Calgary, Alberta, using a variety of flow visualization techniques to provide a qualitative assessment of supply air movement from the diffusers [14]. They concluded that the mechanical system was "generally performing adequately," however, operating and layout characteristics of the air distribution system and the positioning of partitions in the office created some areas where negligible air movement was observed. Based on their

observations in the building, PWC recommended that partitions be raised slightly off the floor to provide good air circulation. Subsequently, PWC documented in detail their methods for evaluating air circulation in buildings [15]. Huvinen and Rantama tested ventilation efficiency in a 3 m x 3 m (10 ft x 10 ft) partitioned office space within a larger open plan office [16]. Theoretical predictions and a limited amount of experimental data showed little difference between 1.5 m (5 ft) and 2.0 m (6.6 ft) high partitions. In the same study, significant differences in air circulation were predicted by the model when a gap was provided at the bottom of the partitions, but no experimental data were presented to verify this result. The results were strongly dependent on the inlet/outlet configuration and the control objectives of the mechanical system. In a recent publication, Nguyen reported on full-scale testing of ventilation effectiveness for office partitions of two different heights (48 in. and 62 in.) and that were raised above the floor by 3, 6, 9, and 12 inches [17]. Although it was concluded that "depending on the type of diffuser, raising the partitions above the floor at a certain elevation does provide a better fresh air exchange rate," and "the height of partitions ... has an impact on air exchange rates and air velocities," there were not enough experimental data reported from which to accurately understand the rationale behind these statements.

In the current study, a series of detailed laboratory experiments were carried out to investigate the effects of office partition configurations and environmental control parameters on thermal and ventilation conditions within workstations. The range of partition and environmental parameters investigated included: (1) partition height, (2) solid vs. airflow partitions, (3) airflow gap size, (4) supply air volume, (5) supply/room temperature difference, (6) supply diffuser location, (7) heat load density, (8) workstation size, and (9) cooling vs. heating mode. The current effort did not include modeling by either detailed numerical or simplified methods in order to address the fundamentals of the airflow conditions under study. Future work is planned in this area.

The overall objectives of the study were to:

1. Evaluate the conditions under which partition designs can improve or degrade air movement, ventilation performance, and worker comfort; and
2. Evaluate the effects of the Steelcase airflow partition on air movement, ventilation performance, and worker comfort.

EXPERIMENTAL METHODS

Controlled Environment Chamber

All experiments were performed in a controlled environment chamber (CEC) measuring 18 ft by 18 ft by 8 ft, 4 in. (5.5 m by 5.5 m by 2.5 m) and located in the Building Science Laboratory, Department of Architecture, University of California, Berkeley, California. The CEC is designed to resemble a modern office space while still allowing a high degree of control over the test chamber's thermal environment [18]. The floor is fully covered with carpet tiles, the finished gypboard walls are heavily insulated and painted white, triple-pane windows in the two exterior walls provide a view to the outside, the suspended ceiling contains patterned acoustical tile, and six 2 ft (0.6 m) square recessed dimmable lighting fixtures are mounted in the ceiling. As shown in Figure 1a, a raised access floor system provides a 2 ft (0.6 m) high subfloor plenum, and the suspended ceiling provides a 1.5 ft (0.5 m) ceiling plenum.

A typical modular office configuration was installed in the test chamber using Steelcase Series 9000 systems furniture. As shown in Figure 1b, the partitions were set up to produce two small 60 in. by 75 in. (1.5 m by 1.9 m) workstations, and one double-sized 120 in. by 75 in. (3.05 m by 1.9 m) workstation. The arrangement of furniture, including desks, side tables, and overhead storage bins, is also shown in the figure. The base-case partition configuration used during a large majority of the tests consisted of medium-height (65-in. [1.65 m]) airflow partitions. Figure 2a shows the locations of the airflow and solid partitions; airflow partitions were installed everywhere except along the 30-in. (0.76 m) sides of the desks, where the desk support would completely block any airflow gap. In order to take advantage of airflow partitions placed along the back of each desk and side-table, all modesty panels (vertical panel on backside of desk) were removed.

To aid the experimental method for comparing the performance of solid vs. airflow partitions, replacement panels for each airflow gap were fabricated out of 1/4-inch foam core. Velcro strips placed on the back of each panel allowed it to be positioned to completely cover the airflow gap (forming a solid partition), or to be easily secured to the fabric of the partition to produce a full-sized or partial-sized airflow gap (Figure 2b). Also shown in Figure 2b are 10-in. (0.25 m) extension panels which were designed and

fabricated to fit on top of the 65-in. partitions, thereby increasing the overall partition height to 75 in. (1.9 m). These extension panels allowed us to quickly convert the office configuration from medium-height to tall partitions, improving the comparability of measurement results obtained under similar thermal conditions. The extension panels also allowed us to investigate the effects of the airflow gap in tall 75-in. partitions.

The CEC's reconfigurable air distribution system permits ducted or plenum air to be supplied to and returned from the test chamber at any combination of ceiling and floor locations. Figure 1a shows the airflow configuration used during the tests reported here, consisting of a conventional ducted ceiling supply-and-return air distribution system. Figure 3 describes the various locations of the supply diffuser(s) and return register used during the tests in relation to the nine by nine grid of 2 ft by 2 ft (0.6 m by 0.6 m) suspended ceiling panels. During most tests supply air was provided through a single perforated lay-in diffuser*, positioned near one side of the room at (x=5, y=2). At this position, the internal pattern deflectors were adjusted to produce a 3-way airflow pattern, away from the adjacent wall, as shown in Figure 3. A single perforated return register was located at (5,9) during all tests. By placing supply and return locations at opposite sides of the room, airflow conditions in the central region of the test chamber were expected to resemble those encountered in open plan offices, where most workstations are positioned somewhere between supply and return locations. Figure 3 also shows the alternative diffuser locations and blow configurations that were studied during a series of additional tests that will be discussed later in *Results and Discussion.* These include: (1) single diffuser at (8,5) with 3-way blow away from window; (2) single diffuser at (2,8) with 2-way blow away from adjacent corner of room; (3) single diffuser at the base case position (5,2) with 3-way blow away from window; and (4) two diffusers at (2,2) and (8,2) with 2-way blow away from the adjacent corners.

The CEC air distribution system also allows a separately controlled airflow to be provided within the plenum wall construction of the two exterior chamber walls and between the inner two window panes called the annular space. During most tests, airflow through the annular space maintained the temperature of the interior window pane at approximately the average indoor air temperature. Consequently, the exterior walls and

*Model PDL, Environmental Technologies, Largo, FL.

windows were not a source of strong natural convection airflow, but affected indoor air movement like interior walls. During heating-mode tests in the chamber, cooled air was passed between the windows to simulate cooling effects in the perimeter zone of an office space.

Heat loads were provided to simulate typical office load distributions and densities. Overhead lighting fixtures had a total power rating of 500 W (1700 Btu/h). Energy balance tests indicated that only a small fraction (≈100 W [340 Btu/h]) of the overhead lighting load contributed to the room load. Personal computers, containing small internal cooling fans, and monitors (≈90 W [310 Btu/h] total) were placed on each of the three desktops. Each workstation had a 75 W (256 Btu/h) task light above the desk. During the thermal measurements, a second 75 W light bulb was located at the 1.1 m level near the edge of the desk to simulate the sensible heat load from a typical office worker. The experimenter and computer-based data acquisition system also added approximately 150 W (510 Btu/h) to the total load during these tests. During the tracer gas measurements, one or two of the three workstations was occupied by a seated mannequin. Electric resistance heating elements wrapped around the mannequin released 75 W in a manner that closely resembled the sensible heat load of an office worker. Two different office heat load densities were studied during the thermal experiments. The heat sources described above generated a load density of approximately 35 W/m^2 (11 Btu/h·ft^2). A higher load density of 55 W/m^2 (18 Btu/h·ft^2) was produced by placing a 200 W (680 Btu/h) electric radiant heater on the floor under each desk to represent larger computer processing units. Most of the tracer gas tests were performed at the lower heat load density of 35 W/m^2. During a few tests, internal loads were increased by operation of mixing fans within the chamber. In tests with the chamber heated using warm supply air, the only additional heat gain to the space was from the overhead lights.

Except for a few heating-mode tracer-gas tests, all experiments were carried out under steady-state conditions chosen to represent an interior zone of an office building. To achieve these conditions the electrical heat sources in the room and the mechanical system were turned on in the morning and allowed to warm up the room until the expected average room temperature for the upcoming experiment was reached (22°C to 28°C [72°F to 82°F] during these tests). After completing the warm-up, the supply air volume and temperature were adjusted to their selected setpoints, and conditions in the

room were allowed to further stabilize. Typical control of the supply air temperature entering the room was to within ±1.0°C (1.8°F) over the test period. Room humidity levels were not controlled during the tests.

Heating mode tests were initiated with a similar cool-down period during which cool air was passed through the annular space until the windows reached a steady minimum temperature (≈13°C [55°F]). After the warm supply air temperature and volume into the test chamber were set and stabilized, the test proceeded under steady-state conditions.

Thermal Measurements

Detailed air velocity and temperature measurements within the test room were accomplished by using a lightweight sensor rig fabricated of aluminum tubing that allowed a vertical array of sensors to be positioned at desired measurement heights and moved around the room to map out a grid of selected measurement locations (Figure 4). By positioning the sensors within the space defined by the structural elements of the rig, protection was provided against damage from accidental encounters with office furniture and other obstacles. At each location in the room, air velocity and temperature were measured at six heights: 4 in. (0.1 m); 2 ft (0.6 m); 3 ft, 7 in. (1.1 m); 5 ft, 7 in. (1.7 m); 6 ft, 7 in. (2.0 m); and 7 ft, 9 in. (2.35 m). The 0.1-m, 0.6-m, and 1.1-m levels correspond to recommended measurement heights for seated subjects, and the 0.1-m, 1.1-m, and 1.7-m levels correspond to heights recommended for standing subjects, as specified by ASHRAE [3]. Figure 5 shows the twenty-six measurement locations that were used during most of the tests. They include 4 points each in workstations #1 and #2 (WS#1 and WS#2), 12 points in WS#3, and 6 additional points in the surrounding corridors.

Velocities were measured with spherical-element omnidirectional anemometers having a range of 0 to 600 fpm (0 to 3 m/s), and temperatures were measured with shielded thermistor temperature probes. All sensors were calibrated prior to testing. An 11-point anemometer calibration was performed over the range of 0 to 80 fpm (0 to 0.4 m/s) using a precision calibration unit. Although this represented a small portion of the total range of the probes, it covered the range of velocities most commonly measured in the subsequent experiments. Calibration curves produced for each anemometer were found to agree with the calibration standard to within ±4 fpm (±0.02 m/s) over the range tested.

Each temperature sensor was calibrated by placing it in an ice bath and adjusting its output (if necessary) to the reference voltage level. A subsequent side-by-side comparison of all sensors at room temperature found agreement to within ±0.2°F (0.1°C).

A portable computer-based data acquisition system was used to record the readings from the velocity and temperature sensors mounted on the aluminum sensor rig. After positioning the sensor rig at the desired measurement location, all twelve sensors were sampled 50 times over a 90-second measurement period. The rig was then moved to the next measurement location and the measurements repeated. At the end of each sampling period, the system calculated and stored average, maximum, minimum, and standard deviation values for each sensor. Approximately two minutes were required to complete the measurement procedure at each location, so that a complete test generally took between one and two hours, depending on the number of measurement locations (typically 26). After the test was completed, the data were transferred to a spreadsheet for further analysis.

Supply and return air volumes were monitored with a high-precision flow measurement setup consisting of a series of small-diameter (3-4 in.) PVC pipes with pitot tubes mounted to measure the fully developed flow. The volume of supply air entering the test room through the ceiling diffuser was checked and balanced with a flow hood. Tests to measure the air velocities at less accessible points in the room (e.g., air passing through the partition airflow gap) were performed with an elliptical-element omnidirectional anemometer. Flow visualization of the room airflow patterns was performed with a neutral-density bubble generator.

Additional temperature measurements in the ducts and room were made with thermistor elements contained in duct immersion or wall-mounted units. These, along with other parameters, were monitored and recorded through the PC-based direct digital control system for the CEC. Such variables as supply air temperature and volume, average room temperature and humidity, return air temperature, annular space temperature, and outside air temperature and humidity were sampled and recorded at 1-2 minute intervals. Globe temperature was measured with a 1.5 in. (38 mm) diameter table tennis ball, as described by Benton et al. [19]. Room surface temperatures were scanned with an infrared thermometer.

Table 1 lists the thermal measurement test conditions. A total of 39 separate tests were completed, including 6 preliminary tests (P1A-P3B), and 33 final tests (1A-16). The tests investigated the following ranges of test parameters: (1) supply air volume from 54 cfm (0.2 cfm/ft^2) to 320 cfm (1.0 cfm/ft^2); (2) heat load densities of 35 and 55 W/m^2 (11 Btu/h·ft^2 and 18 Btu/h·ft^2); (3) supply air temperature from 12.8° to 19.5°C (55° to 67°F) ; (4) average room temperature from 21.9° - 28.5°C (71° to 83°F); (5) return/supply air temperature difference from 5.6° to 12.3°C (10° to 22°F); (6) 75-in., 65-in., 42-in., and 0-in. (no partitions) partition heights; (7) solid partitions, full-open (12-in.), 4-in., and 2-in. airflow gaps.

The final tests listed in Table 1 can be divided into two groups according to supply volume: (1) low supply volume in the range of 150 to 180 cfm (0.5 cfm/ft^2), and (2) high supply volume in the range of 280 to 320 cfm (0.9 to 1.0 cfm/ft^2). At the low supply air volume, the throw of the supply diffuser was at the minimum level recommended by the manufacturer to achieve acceptable room air diffusion. The results of these tests are therefore indicative of a single VAV diffuser operating at or below its minimum airflow rate. At the higher supply air volume, the duct diameter of the neck leading into the diffuser had to be increased from 6 inches (low volume tests) to 10 inches. This modification kept the noise generated by the diffuser to a level less than NC = 35, and provided a throw within the acceptable range for good room air diffusion. Note that the room temperature reported in Table 1 was measured at a typical wall thermostat location and, due to the effect of the warm adjacent wall, is quite close to the return air temperature. For a given supply air volume, the return air volume was adjusted to maintain a slight overpressure in the test room in relation to the surrounding rooms of the building. Due to the relatively high ambient pressure in the surrounding spaces, the return air volume was always less than the supply air volume.

Tracer Gas Measurements

The tracer gas stepup procedure [20-22] was used to study indoor airflow patterns and the spatial variability of ventilation. In this procedure, the supply air was labeled with a tracer gas and the rate of increase of tracer gas concentrations at a location indicated how rapidly the indoor air was replaced with outdoor air that entered the building since the start of tracer gas injection. During the stepups, a mixture of 1% sulfur hexafluoride SF_6

in air was injected at a constant rate into the supply airstream. A peristaltic pump drew the tracer/air mixture from a storage bag and directed the mixture through a flowmeter and tubing into the supply duct. The injection rate was monitored using rotameters calibrated with a bubble flowmeter and was generally stable within ±2%. To ensure thorough mixing of the SF_6 in the supply airstream, an array of small propeller fans was installed downstream of the injection point. These fans were oriented to cause air flow perpendicular to the general direction of flow in the duct. Mixing was confirmed by collection and analysis of air/tracer samples. Air samples were drawn continuously through copper tubes to three gas chromatographs (GCs) equipped with electron capture detectors. During Tests 21-25, five samples originated from within the chamber at a subset of the locations illustrated in Figure 6 and four samples originated from the HVAC system. During Tests 39-46, one sample originated from within the chamber and four samples originated from the HVAC system. The GCs were capable of analyzing a sample within 1 minute using: a 0.38 m long molecular sieve main column; a backflush column with two sections (0.08 m of 5% phosphoric acid on Chromosorb GAW followed by 0.38 m of molecular sieve); carrier gas (5% methane, 95% argon) flow rates of approximately 40 cc/min; and approximately a 12 s backflush time [23]. Using this method, the tracer gas concentration was measured every three minutes at each sample location. The time required to perform repeated real time tracer gas measurements limited the maximum supply air volume (200 cfm) for which reliable test results could be achieved. As a result, as seen in Table 2, most tracer gas tests were performed at a low supply volume of 100 cfm (0.3 cfm/ft^2).

During the tests, bag samplers also directed air/tracer samples at a constant rate into 0.75 L sample bags. Bag sampling commenced at the start of tracer gas injection and continued until tracer gas concentrations were stable (as determined from the periodic measurements of tracer gas concentration in the return duct) at which time syringe samples were collected manually from each location. The fourteen (Tests 21-25) or seventeen (Tests 39-46) bag samplers collected samples from the locations within the chamber depicted in Figure 6. Air samples were directed to both a sample bag and a GC at some locations, thus, samples were collected and analyzed from 17 unique locations within the CEC. Bag and syringe samples were analyzed using the GCs immediately after completion of the tests. Equipment and procedures are similar to those used previously and described by Fisk et al. [21,22,24].

The GCs were calibrated prior to each test using nine total calibration gases with SF_6 concentrations of 0 ppb to 185 ppb. Measurements of tracer gas concentrations were generally repeatable within a couple ppb.

Since the tracer gas measurement methods required the test chamber to be closed and unoccupied throughout each test, tracer gas tests were performed on separate days from the thermal tests described in Table 1. Table 2 lists the tracer gas test conditions. There is no relationship between test numbers for Tables 1 and 2. Gaps in the sequence of test numbers are due to tests with air supplied through floor units or unsuccessful tests. During Tests 21-25, the supply diffuser was centrally located at position (5,4) (see Figure 3) and adjusted for a 4-way 360° air supply orientation. During Tests 39-46, the supply diffuser was located at position (5,2) and adjusted for a 3-way 270° air supply orientation with no air directed toward the windows. Test variables included: partition height, absence or presence of a 0.3 m (12 in.) gap at the bottom of the partitions, supply flow rate, supply temperature and internal heat loads. In most tests, the CEC was cooled to offset the internal heat loads. During Tests 23, 43, 45 & 46, the windows were cooled, internal heat generation was reduced, and the supply air was used to heat the chamber. To determine measurement precision, Tests 22W and 42W were run with fans operating in the chamber to vigorously mix the chamber air. Test 22 was a tracer gas decay (instead of stepup) with the tracer gas concentration uniform at the start of the decay and no tracer injection during the decay.

Tracer Gas Data Analysis

Age of air concepts are a common basis for evaluating ventilation efficiency and the spatial variability of ventilation in a ventilated space. The age of air in a sample collected at a specific location, is the time that has elapsed since the air entered the building. The reciprocal of the age of air is a measure of a local ventilation rate. Thus, a relatively low age of air indicates a higher rate of ventilation than a relatively high age of air. Equations based on age distribution theory [20] were used to calculate the ages of air. We present only the equations for a tracer gas stepup; similar equations for data from tracer gas decays are presented elsewhere [20]. Using tracer gas concentrations as a function of time, the following equation was employed:

$$A = \int_0^{t_{ss}} [1 - C(t)/C(t_{ss})]\, dt$$

where: A is the age of air, t is the time variable set equal to zero at the start of tracer gas injection, C(t) is the tracer gas concentration at time t, and t_{ss} is the time when concentrations have stabilized. The integral is evaluated numerically. Using the tracer gas concentrations in bag and syringe samples, C_{bag} and C_{syr}, respectively, age of air was determined using the equation:

$$A = t_{bag}\,(1 - C_{bag}/C_{syr})$$

where t_{bag} is the elapsed time of bag sampling.

To indicate the spatial variability in the age of air, we use the age expressed in hours, and various ratios based on the ages. For example, the age of air in the return duct divided by the average age of air in all of the workstations at 0.4 m and 1.1 m above the floor yields a ratio that is an indicator of short-circuiting. With short-circuiting, fresh (low age) air does not mix thoroughly with room air before exiting via the return duct. Therefore, values less than unity for this ratio indicate short-circuiting since the age of air in the return is lower than the age in the workstations. When ratios contain an average of the age measured at several locations, we use volume-weighted averages assuming that each measurement is representative of a volume that extends half way to adjacent measurement points and/or to the edge of the workstation.

RESULTS AND DISCUSSION

Thermal Measurements

Due to the large amount of experimental data, a subset of tests has been selected from Table 1 for presentation and discussion to demonstrate the effects of each of the major test parameters investigated. The emphasis of the data presented here is on the local thermal conditions within each workstation. For brevity, average conditions at a given height in a workstation are defined below as the velocity or temperature calculated by averaging the measured values obtained from the four locations directly in front of the desk. Referring to Figure 5, average conditions in WS#1 are based on points 13, 14, 15,

and 16, those in WS#2 are based on points 17, 18, 19, and 20, and those in WS#3 are based on points 3, 4, 7, and 8.

Based on preliminary test results indicating that the largest effects, if any, of the airflow gap partition would occur at the highest supply air volumes, a base case set of environmental control conditions was selected and used for a majority of the parametric studies investigating the influence of partition design. These base case conditions consisted of: (1) high supply air volume (0.9 to 1.0 cfm/ft^2), (2) high heat load density (55 W/m^2), (3) supply diffuser location at (5,2) (see Figure 3), and (4) supply air temperature in the range of approximately 17° to 19°C, selected to maintain the average room temperature in the range of approximately 24° to 25°C.

Data Precision. A measure of the experimental repeatability of our thermal measurements is indicated in Figures 7a and 7b, each of which presents velocity results from three tests having similar test conditions. Figure 7a shows results from tests 8C, 9A, and 12B for solid 65-in. partitions under base case conditions. Figure 7b shows results from tests 1A, 2B, and 7C for solid 65-in. partitions at low supply air volume (≈0.5 cfm/ft^2), high heat load density (55 W/m^2), supply diffuser location at (5,2), and a lower supply air temperature of 13°C. In Figure 7a, at the higher supply air volume, the results are repeatable for all three workstations, with all measured velocities in the occupied zone (0.1 - 1.7 m) falling within 0.03 m/s of each other. This is a good result, as there is some variation in the supply air volume and temperature conditions between the three tests, but the test-to-test variability is only slightly greater than the calibrated accuracy of the anemometers. In Figure 7b, at a lower supply volume and temperature, velocities in the occupied zone are repeatable to within 0.05 m/s, except at the 1.7 m level in WS#2. The wider variation in WS#2 is due to the minimum diffuser throw characteristics described earlier.

Solid Partition Height. Figure 8a presents average velocity results for tests 8B, 9A, 15, and 14, corresponding to solid partition heights of 75 in., 65 in., and 42 in., and no partitions, respectively. The tests were performed under base case conditions and the results are organized by workstation. In Figure 8a, results are shown for all six measurement heights (0.1 to 2.35 m). As expected, the highest velocities are recorded at the 2.35 m height, where the sensors are in direct line with the air supplied horizontally

along the ceiling by the supply diffuser. In WS#1 and WS#3, which are located closer to the supply diffuser, velocities near the ceiling are between 0.3 and 0.45 m/s, while in WS#2, located further away, these velocities are in the range of 0.15 to 0.25 m/s. This pattern of results was obtained consistently for all tests under base case conditions. Due to the emphasis on thermal conditions within the occupied zone (0.1 to 1.7 m), for the remainder of this report, results will be presented only up to a height of 2.0 m, enabling greater detail to be observed, and an improved comparison to be made between separate measurements at lower heights in the room.

Figure 8b shows the results of Figure 8a replotted for the measurement heights from 0.1 to 2.0 m. The observations are as follows:

1. The largest differences between tests occur in WS#1, due to its proximity to the supply diffuser. Within WS#1, the no-partition test shows the highest velocities at all measurement heights, although the differences are only significant at the 0.1 m and perhaps the 0.6 m levels. The next highest air velocities at these same two heights occurred for 75 in. partitions, and decreased with decreasing partition height to their minimum values for 42 in. partitions. The upward entrainment of air by the overhead supply diffuser, combined with the buoyancy-driven airflow produced by the high heat loads within the partitioned workstation generated these characteristic velocities.
2. In WS#2, the no-partition test again seems to have the highest overall velocities, although this result is not as significant as it was in WS#1. Velocity differences caused by partition height effects are quite small and follow no observable pattern.
3. In WS#3, velocity differences between all four tests are insignificant. This result is not surprising, as the magnitude of partition effects should diminish with increasing workstation size, approaching, in the limiting case, air movement conditions found with no partitions present.

Partition Height and Gap Size. Figure 9 presents average velocity results for tests 8A, 8B, 8C, 9B, 9C, and 12A, comparing the effects of solid and airflow partitions for both 65-in. and 75-in. heights under base case conditions. As previously described, the tall airflow partitions were formed by placing 10-in. extension panels on top of the 65-in. airflow partitions (see Figure 2b). Two gap sizes were investigated: (1) full open, and (2) 4-in. gap located above the steel cross-member of the partition -- in this case, the 2-in gap

between the floor and the cross-member (typically used for the electrical powerway) was covered. The observations are as follows:

1. Overall, the results show only small differences in velocities between solid and airflow partitions, and in most instances, the measured differences are experimentally insignificant.
2. The largest observed effects occur at the 0.1 m level in WS#1 for 75-in. partitions and at the 1.1 m level in WS#2 for 65-in. partitions. For these cases, a 70-100%, or 0:08 m/s (16 fpm), increase in velocity was obtained between solid and airflow partitions. Even so, the velocities for solid partitions were so low that all velocities from all tests were still within the comfort zone limits specified by ASHRAE Standard 55-81 [3].
3. Except for results for the 65-in. airflow partition in WS#2, measured velocity differences are insignificant at the 0.6 m level and above. This result supports the conclusion that in most instances airflow partitions appear to provide little or no comfort benefits to an office worker, who will be most sensitive to changes in velocity at the head level (1.1 m). Overall comfort results are discussed later.
4. There are no identifiable effects of the 4-in. gap in comparison with the solid partition for all three workstations.
5. In the large majority of cases, there are no differences between 65-in. and 75-in. partitions.

Partition Air Gap. Figures 10a and 10b show average velocity results for tests 5A, 5B, 6A, and 6B. All test conditions were the same as those for the base case, except for a lower supply air temperature of 13° to 15°C. Four different airflow gap configurations for the medium height (65-in.) partitions were investigated: (1) solid; (2) open (12-in airflow gap); (3) 2-in. airflow gap, formed by covering all of the airflow gap except the 2-in. opening between the floor and the steel cross-member; and (4) combination, in which all airflow gaps are full open except in the two 60-in. partitions separating WS#1 and WS#2 from WS#3, which remained covered. In Figure 10a, the results are organized by workstation, and in Figure 10b, they are organized by air gap configuration. The observations are as follows:

1. The pattern of results is very similar to those presented in Figure 9.
2. The largest observed effect occurs near the floor level in WS#1, where an increase of

nearly 200%, or 0.15 m/s (30 fpm), was obtained at the 0.1 m level between the solid and combination partitions.

3. The floor-level velocity differences due to the airflow partition are greatest in WS#1, which is the closest to the supply air diffuser. The magnitude of these differences is also greater than that found in Figure 9, due in part to the colder supply air temperatures used in tests 5 and 6. Colder supply air temperatures (larger supply air /room air temperature differences) increase the movement of air down to the floor level.
4. The slight increase in air motion occurring at the 0.6 and 1.1 m levels in WS#2 for open airflow partitions is nearly identical to that observed in Figure 9. This effect is not seen in the larger WS#3, so it appears that airflow partitions may provide small increases in velocity within small workstations. The precise relationship between the magnitude of this effect and distance to the supply diffuser requires further investigation.
5. The smaller 2-in. airflow gap provides the same trends in air movement as the larger 12-in. airflow gap.
6. The larger workstation (WS#3) has slightly higher average air velocities than WS#1 and WS#2 under most test conditions (Figure 10b). The one exception is the open airflow partitions, for which no discernible difference among the three workstations is observed.

Figure 10c presents average temperature results for the same four tests (5A, 5B, 6A, and 6B). The observations are as follows:

1. The ceiling diffuser does a good job of mixing the room air with no significant stratification measured in any workstation for all test configurations.
2. All measured temperatures are within the ASHRAE-specified winter or summer comfort zones [3].
3. Temperature differences between separate tests are largely accounted for by the different average room temperatures maintained during each test (see Table 1). For example, test 5A (solid partition) had the highest supply air and room air temperatures, and correspondingly demonstrates the highest workstation temperatures in Figure 10c.

Supply Air Volume and Temperature. Figures 11a and 11b present average velocity and temperature results, respectively, for five different combinations of supply air volume and temperature (tests 3A, 6C, 7C, 9A, and 12B). Solid 65-in. partitions, high heat load density, and the base case diffuser location were used in all five tests. The observations are as follows:

1. In WS#1, there is only a small overall effect on velocity with the maximum difference between all test results at all measurement heights being no greater than 0.04 m/s (8 fpm). At the lower measurement heights, tests using higher air supply volumes (6C, 9A, and 12B) provide slightly higher velocities.
2. In WS#2 and WS#3, the measured velocity differences are also quite small. In most cases, the highest velocities at the lower measurement heights (0.1 to 1.1 m) are provided by the two tests using the lower supply air temperature (tests 6C and 7C). This result is consistent with the improved buoyancy-driven mixing that should result for larger supply/room temperature differences.
3. Temperature data in Figure 11b again exhibit negligible stratification in the room.
4. Temperature differences between tests demonstrate a consistent pattern in all three workstations, with a 3°to 3.5°C (5.5° to 6.5°F) difference between the maximum and minimum results.
5. The lowest temperatures are provided by a high supply air volume combined with a low supply air temperature (test 6C), while the highest temperatures are provided by a low supply air volume combined with a high supply air temperature (test 3A). The other three tests (high supply volume with high supply temperature, and low supply volume with low supply temperature) produce intermediate temperature results of similar magnitude.

Supply Air Volume and Partition Gap. Figures 12a and 12b present average velocity results in WS#1 for tests 1A, 1B, and 2A (0.5 cfm/ft^2) compared to tests 5A, 5B, 6A, and 6B (1.0 cfm/ft^2). All tests used a low supply air temperature (13° to 15°C), and four different airflow gap configurations were investigated: (1) solid, (2) open, (3) 2-in., and (4) combination. In Figure 12a, the results are organized by supply air volume, and in Figure 12b, they are organized by partition configuration. The observations are as follows:

1. The effect of supply air volume appears to be quite small, as average air velocities increase only slightly at a few measurement locations. Maximum increases at the higher supply air volume were on the order of only 0.05 m/s (10 fpm).
2. In Figure 12b, results for all three partition configurations were nearly identical for both supply air volumes.

Diffuser Location. Figure 13 shows velocity results for a series of tests investigating the effects of four alternative supply diffuser locations for both solid and airflow partitions. Refer to Figure 3 for the diffuser locations tested, which included: (1) single diffuser at (8,5) with 3-way blow away from window (tests 10A and 10B); (2) single diffuser at (2,8) with 2-way blow away from adjacent corner of room (tests 11A and 11B); (3) single diffuser at the base case position (5,2) with 3-way blow away from window (tests 12A and 12B); and (4) two diffusers at (2,2) and (8,2) with 2-way blow away from the adjacent corners (tests 13A and 13B). All tests were performed under base case conditions, except for changes in the diffuser location. In the figure, results for solid partitions are plotted with a solid line, and results for airflow partitions are plotted with a dashed line. Velocity data for the 2.35 m height are also included due to the strong dependence of airflow near the ceiling on diffuser location. The observations are as follows:

1. In WS#1 for test 10, significantly higher velocities (0.3 to 0.35 m/s [60 to 70 fpm]) are obtained at the 1.1 m height. The absence or presence of airflow partitions has no influence on the nature of these results.
2. Although smaller in magnitude, higher velocities are observed at lower heights (0.6 and 1.1 m) in WS#2 during test 12A. In test 12, however, higher velocities at these locations are only observed for airflow partitions (test 12A) and not solid partitions (test 12B).
3. In test 11, the supply diffuser was positioned in the corner of the test room near WS#2. As expected, high air velocities (0.5 m/s [100 fpm]) are obtained near the ceiling in WS#2. No significant differences between solid and airflow partitions are observed in all three workstations. This observation is important because it is contrary to previously obtained results for the base case test configuration, in which the largest partition effects were found in WS#1, due to its proximity to the supply location. The closeness of the return register to the supply location may account for

some of the differences found in test 11.

4. In test 13, with two supply diffusers, the highest ceiling-level velocities are obtained in WS#1 and WS#3, the two closest workstations. The airflow partitions have a relatively minor effect in all workstations, except at the 0.1 m level in WS#1, where a 100%, or 0.09 m/s (18 fpm), increase is measured.
5. Overall, WS#2 is the only workstation with a consistent pattern of slightly elevated air velocities in the seated occupant zone (0.1 to 1.1 m) for airflow partitions compared to solid partitions. The one exception to this pattern was obtained when the supply diffuser was positioned in the corner near WS#2.
6. There is no distinct pattern of airflow vs. solid partition effects in WS#1 and WS#3.

Heat Load Density. Figures 14a and 14b present average velocity and temperature results for tests 1A, 1B, 4A, and 4B. Test 1 was performed with high heat loads (55 W/m^2) and Test 4 with low heat loads (35 W/m^2). Both tests were performed at the lower supply volume (0.5 cfm/ft^2) and lower supply temperature (13°C). As above, results for solid partitions are plotted with a solid line, and results for airflow partitions are plotted with a dashed line. The observations are as follows:

1. In Figure 14a, there are no observable heat load effects, except at the 0.6 and 1.1 m levels in WS#3, where slight increases in velocity (0.03 to 0.08 m/s [6 to 16 fpm]) are obtained for the higher heat load. These differences are greatest (100% increase) when comparing solid partition test results.
2. The existence of airflow partitions has no noticeable effect, except at the 0.1 m level in WS#1, where small velocity increases occur, similar to previously discussed results.
3. The effects of heat load density on temperature are clearly evident in Figure 14b, where a 2°C (4°F) temperature difference exists between tests 1 and 4. There is no measurable stratification in the room, as previously observed in other temperature results. The existence of airflow partitions has a negligible effect on temperature distributions in all workstations.

Air Diffusion Performance Index. ASHRAE Standard 113-90 [1] provides a method for evaluating the ability of an air distribution system to produce an acceptable thermal environment, based on air motion and air temperature distribution. The air diffusion

performance index (ADPI) is a calculated quantity representing the percentage of measurement locations where velocities and temperatures meet certain criteria in terms of magnitude and uniformity. The air diffusion performance of a system is considered acceptable when an ADPI of 80% or greater is obtained.

Table 3 presents calculated ADPI results for 17 tests selected to cover the full range of test conditions. Eighty points within the three workstations were used for each calculation, consisting of the four heights in the occupied zone (0.1 to 1.7 m) for location numbers 1-20, as shown in Figure 5 (4 locations each in WS#1 and WS#2, and 12 locations in WS#3). The test conditions covered were: (1) low (5-6 cfm/m^2) and high (10-11 cfm/m^2) supply air volume (SAV), (2) low (35 W/m^2) and high (55 W/m^2) heat load density, (3) low (13°-15°C) and high (18°C) supply air temperature (SAT), (4) no, 42-in., 65-in., and 75-in. partitions (Part), and (5) solid (S) and full open airflow (O) partitions.

The air diffusion performance for all tests is quite acceptable, as calculated ADPI values ranged from 89% to 99%. The largest difference between solid and airflow partitions occurred in test 8, for which the ADPI increased from 90% to 98% for the solid and airflow partitions, respectively. This difference is not considered significant due to the already excellent ADPI for the solid partitions. Our conclusion from the results of Table 3 is that the air diffusion performance within the workstations is essentially identical for all tests.

Air Gap Velocities. As a further test of the characteristics of the air movement through the gaps in the airflow partitions, a series of hand-held velocity measurements were made of the air as it passed through the openings in the partitions. Figure 15 identifies the seven locations where air gap velocities were recorded for the conditions of test 12A. Five different gap sizes were investigated by positioning the removable panel as shown in Figure 2b(f). The 2-in. gap was formed by covering everything except the space between the floor and steel cross-member of the partition. All other gap sizes were formed by covering the 2-in. gap at the floor and adjusting the panel to cover the desired portion of the 10-in. gap above the steel cross-member. The velocity sensor was placed near the bottom of the airflow opening at the center of the partition.

Table 4 lists the measured air gap velocities. The highest velocities for all gap sizes are consistently recorded at locations 1 and 4, which are the closest partitions to the supply diffuser. Gap velocities at location 2, separating WS#1 and WS#2, are also nearly as high as those found at location 4. However, no clear relationship between velocities and gap size is observed.

A qualitative assessment of the air motion through the partition gaps at locations 1, 2, and 3 was performed using a helium bubble machine. Figure 16 presents the observed flow patterns in WS#1 and WS#2 for the conditions of test 10. The supply diffuser was located at position (8,5) (see Figure 3) during this test. Figure 16a shows the results for test 10B with solid partitions. Most of the supply air from the diffuser reached the walls and some went directly to the return register. Within both workstations the airflow was primarily upward, driven by the local heat sources and fed by air moving through the entrance to the cubicle. Figure 16b shows the results for test 10A with airflow partitions. Air near the floor on the right side of the chamber was observed to pass through the partition gap into WS#1. This appeared to aid in the noticeably higher rate of air movement in WS#1 compared to WS#2. Some air flowing along the floor in WS#1 was observed to pass on through the partition gap into WS#2, but at a lower rate compared to the airflow into WS#1 at location 1. In WS#2, no obvious direction of flow was evident through the partition gap on the left (location 3). Air movement within WS#2 was not significantly affected by flow through the air gaps, and remained primarily upward, as in Figure 16a. In general, the flow visualization results supported the gap velocity data reported in Table 4.

Thermal Comfort. The Fobelets and Gagge two-node comfort model [2] was used to predict the characteristic comfort indices for a selected number of tests. The model accounts for the combined effects of air temperature, air velocity, mean radiant temperature, relative humidity, clothing level, and activity level. The measured data used as input to the model consisted of: (1) air temperature and velocity data averaged for the 0.1, 0.6, and 1.1 m levels directly in front of each desk, representing a whole-body average for a seated worker, and (2) globe temperature measured at the 1.1 m level near the front edge of the desk, allowing the calculation of mean radiant temperature. The other three inputs to the model were assumed constant values, representing typical conditions for sedentary office work: (1) 50% relative humidity, (2) 0.5 clo, and (3) 1.2 met.

The comfort model predictions for effective temperature (ET*), discomfort index (DISC), and predicted mean vote (PMV) are listed in Table 5. The observations are as follows:

1. Comfort conditions in all three workstations for tests 11 and 12 (65-in. partitions) are at or above the upper limit (ET* = 26°C [79°F]) of the comfort zone, as specified by ASHRAE Standard 55-81 [3]. These results were obtained despite the maintenance of air temperatures in the range of 23.5° to 25°C (74° to 77°C) within all workstations during these tests. The uncomfortably warm comfort predictions reflect the significant impact of the high heat load levels on radiant temperatures in the workstations.
2. For tests 11 and 12, the most acceptable comfort conditions are obtained in the larger WS#3. Each workstation contains the same magnitude of heat sources, thus generating higher mean radiant temperatures within the smaller WS#1 and WS#2.
3. No comfort improvements are predicted for airflow partitions (tests 11A and 12A) in comparison with solid partitions (tests 11B and 12B). This is an important result because during test 12, the largest overall velocity increases due to airflow partitions were recorded. Measured velocities at the 0.1 to 1.1 m heights in WS#2 were 0.05 to 0.07 m/s (10 to 14 fpm) higher (100% increase) for airflow partitions compared to solid partitions (see Figure 13). Despite the improved air motion, no significant comfort benefits were predicted.
4. As expected, comfort conditions are identical in all three workstations when no partitions are present (test 14). The absence of the heat absorbing partitions also reduces the mean radiant temperatures, producing thermal conditions within the ASHRAE comfort zone.
5. A comparison of results for tests 15 and 16 (42-in. partitions) demonstrates the important influence of supply air temperature. Except in WS#3, conditions are too warm during test 15, which had a high supply air volume and temperature. Test 16, however, produces considerably improved comfort conditions, even though it was performed with a supply air volume of about half that used in test 15. The major reason for this improvement is the cooler supply air temperature (13°C [55°F]) in test 16. WS#1 experiences perfectly neutral comfort conditions (ET* = 24°C, DISC = 0.0, PMV = -0.02) and WS#3 is also predicted to be quite comfortable. WS#2 is noticeably warmer, indicating that the lower supply air volume may have trouble

adequately conditioning small workstations located further away from the supply diffuser.

Tracer Gas Measurements

Data Precision. The precision of the tracer data is indicated by data from two tests in which the air in the chamber was well mixed and by the repeatability of data from tests run at the same experimental conditions.

During Tests 22W and 42W, the chamber air was mixed vigorously with fans which ideally should produce the same local age of air at every point in the chamber and consequently, all of the age of air ratios should equal unity. Table 6 lists the local age of air at all locations measured in the chamber for these tests. Additionally, the average, standard deviation, and coefficient of variation (a measure of relative variability equal to the standard deviation divided by the average) are tabulated. We assume that our measurements of the age of air at a single point are normally distributed. Thus, for a 95% confidence interval, we use twice the largest coefficient of variation (5.3%) or ±11%. Consequently, our estimate of the precision for an age of air measurement is ±11% and smaller differences between two ages of air are not considered significant.

Tests 21 and 22 are comparable tests (run at the same conditions) and produced local ages at all but three locations which were within ±11% of each other. For reasons that are not apparent, Test 21 contains data at two points which are suspect. Therefore, data from Test 22 is used in the subsequent discussion for comparison to data of other tests.

We believe that at least three factors cause imprecision in the multiple (multi-point) measurements of age of air. First, there is a small bias between ages determined from: (a) numerical integration of real-time data, and (b) the bag and syringe samples. We are investigating the cause of this bias. Second, the air in the CEC was probably not perfectly mixed due to the presence of internal partitions. Third, there is undoubtedly some random error in the measured ages due to such factors as instrument imprecision. When we gain more experience and data, a statistical evaluation of measurement precision may become appropriate.

Height Variation in the Age of Air. Table 7 lists average age of air values for the workstations at the knee level, breathing level, near the ceiling level and the return duct. A consistent increase or decrease in the age of air above the floor would be an indication of a general upward or downward air flow pattern. Only in Test 21, (with some suspect data) and Test 40 do the data indicate a consistent trend in age with height (excluding the age at the return duct). These trends are not significant since the average age at the breathing level is nearly identical to the average age at the ceiling level. All other cooling tests show no consistent pattern of age of air variation with height.

Tests 23, 43, 45 & 46 in the heating mode indicate a consistent pattern of age of air with height; however, the variations in age are small (see Figure 17). The ordering of the age of air is, from the lowest to highest, ceiling level, knee level, and breathing level with a maximum percent difference between two levels of 19% (Test 23, from 0.32 hr to 0.38 hr). Since these ages are averages of measurements at several locations, differences greater than 5% are considered significant from the perspective of measurement precision. (In the well-mixed tests, these averages of several ages of air differed by no more than 5%). We have no explanation for this type of pattern in age of air with height.

We have seen no pattern in the age of air with height that is dependent upon the partition height or the presence of a partition gap at the base of the partitions.

Short-Circuiting. Short-circuiting of supply air, for example, air that does not enter the occupied space but travels preferentially to the return, would be evident by ages of air near the ceiling or return duct being lower than ages in the occupied space. Thus, ratios of ages of air near the ceiling or the return to ages of air at the breathing level and knee level should be less than unity for short-circuiting (see Table 8). The values in Table 8 are ratios, therefore our previous measure of data precision is not applicable. Using our precision for an age of air measurement of ±11% for a single point, we calculated the precision of each average value used in the ratios. Using propagation of error analysis [22], we combined the precision values to determine the estimated precisions for each ratio. Thus, the resulting estimated measurement precision for the ratios within the three columns of Table 8 are: ±0.12, ±0.06, and ±0.16, respectively. These estimates of precision should be used to judge whether any value of a ratio is significantly different from unity or whether any two ratio values are significantly different. Ratios from

heating tests (43, 45 & 46) indicate slight short-circuiting and the ratios for Test 23, indicate significant short-circuiting (see Figure 18). Test 23 had the supply diffuser closer to the return than Tests 43, 45 & 46, thus allowing a shorter path for short-circuiting; however, because of the limited data, we can not confirm that the diffuser location was a cause of increased short-circuiting.

Short-circuiting is not evident from the age of air in the aisle for Tests 43, 45 & 46 in which the supply diffuser was relatively far from the aisle. The reason is not clear. Data for Test 21 (a cooling test) yield one ratio less than unity but this result is not consistent with the data from similar tests. Therefore, short-circuiting is only evident in the heating tests.

Workstation Ventilation Uniformity. The preferential ventilation of one workstation over another is a concern to some with regards to partitioned workstations. We have seen no indication of significant preferential ventilation in the configurations tested thus far in the CEC. In Table 9, the maximum difference in ages of air between workstations is less than 20% (Test 45, from 0.80 hr to 0.94 hr, not including Test 21, with suspect data, at 24%). With the supply diffuser moved from a central location to a location farther away from WS#2 and the aisle, there is consistently a slightly higher age of air in WS#2 and the aisle. This relatively higher age of air occurs in WS#2 during both heating and cooling tests. The aisle has a slightly higher age only during cooling tests.

CONCLUSIONS

Measurements were made of the thermal and ventilation performance of a conventional overhead ducted supply-and-return air distribution system in an office environment. The experiments were performed in a controlled environment chamber configured to resemble an open-plan modern office building with modular workstation furniture and partitions. Tests were conducted to investigate the effects of: (1) partition height, (2) solid vs. airflow partitions, (3) airflow gap size, (4) supply air volume, (5) room/supply temperature difference, (6) supply diffuser location, (7) heat load density, (8) workstation size, and (9) cooling vs. heating mode. The major conclusions are as follows:

1. Variations in solid partition height produced only small differences in overall thermal and ventilation performance, although some nonuniformities existed in comparison to an office without partitions. Partition effects, if any, were strongly dependent on the heat loads within the workstation and the proximity of the supply diffuser.
2. For similar test conditions, only small differences in workstation velocities between solid and airflow partitions were obtained, and in the large majority of cases, the measured differences were experimentally insignificant.
3. For the case when the largest overall velocity increases due to airflow partitions were recorded (100% increase in WS#2 during test 12), comfort model predictions indicated no improvement in comfort conditions for airflow vs. solid partitions. Therefore, airflow partitions appear to provide no significant comfort benefits to an office worker.
4. Except for only a few isolated data points, measured velocities at all locations within the occupied zone (0.1 to 1.7 m) for all tests were within the acceptable summer limits specified by ASHRAE Standard 55-81 ($\leq$ 0.25 m/s [50 fpm]) [3]. It is not surprising that changes in velocity at this relatively low range have little effect on overall comfort conditions.
5. The air diffusion performance of the overhead supply-and-return system was quite acceptable and essentially identical for 17 tests selected to cover the full range of test conditions. Calculated air diffusion performance index (ADPI) values ranged from 89% to 99%.
6. Heat loads in partitioned workstations had a significant effect on air temperatures, mean radiant temperatures, and overall comfort conditions. As heat load density (W/m^2) increases (or the workstation size decreases for the same heat load level), thermal conditions will become increasingly warm and uncomfortable, unless other means, such as increasing the air motion or reducing the supply air temperature, are used to provide additional cooling.
7. The location and throw characteristics of the supply diffuser had a significant effect on air motion in nearby workstations. Cooler supply air temperatures demonstrated improved movement of air down to the floor level.
8. The effect of airflow partitions was not significantly dependent on supply air volume. Tests at 0.5 and 1.0 cfm/ft^2 demonstrated only small differences in measured velocities.

9. Reducing the size of the air gaps resulted in lower velocities near the floor relative to velocities obtained for full-sized air gaps. As previously noted, despite the increased velocities, the air gaps had no significant effect on overall thermal comfort.
10. No significant temperature stratification was measured in any workstation for all test conditions.
11. The deviations from uniform ventilation (age of air) noted were slight. This uniformity of ventilation should be checked in field tests of large partitioned office spaces.
12. Short-circuiting of the supply air to the return occurred during heating tests and was absent in cooling tests. Additional tests with heating are required to further evaluate this issue.
13. Partition height and gaps at the bottom of the partitions had little or no effect on the variation of age of air with height, short-circuiting, or uniformity of workstation ventilation.

Due to the acknowledged strong potential influence of room air distribution on thermal comfort and satisfaction, indoor air quality, and worker productivity, future work is needed to address the following important issues:

1. Comparison of field measurements of thermal and ventilation performance in large partitioned offices with test chamber results. In large office spaces, conditions may occur where the predominantly horizontal movement of the bulk air mass between supply and return locations separated by large distances is influenced by obstructing partitions.
2. Additional testing of the effects of heat load density and nonuniform load distribution.
3. Development and testing of alternative Steelcase partition designs for task conditioning.
4. Investigation of the effects of airflow and workstation design on worker productivity.
5. Investigation of the impact of occupant-control and task conditioning on comfort and satisfaction.
6. Development and implementation of detailed room air distribution numerical modeling techniques for addressing the impacts of a wide range of environmental control and workstation design parameters.

ACKNOWLEDGMENTS

We gratefully acknowledge the financial support and generous furniture and partition donations provided by Steelcase, Inc., Grand Rapids, MI. This work was also partially supported by the Assistant Secretary for Conservation and Renewable Energy, Office of Building Technologies, Building Systems and Materials Division of the U.S. Department of Energy (DOE) under Contract No. DE-ACO3-76SF00098. Randy Helm of Steelcase, Inc. served as our technical monitor during this project, and his input, assistance, and understanding were greatly appreciated. We would also like to thank Nora Watanabe of the Center for Environmental Design Research for expertly administering the project.

REFERENCES

1. ASHRAE. 1990. *ANSI/ASHRAE Standard 113-1990*, "Method of testing for room air diffusion." Atlanta: American Society of Heating, Refrigerating, and Air-Conditioning Engineers, Inc.

2. Fobelets, A.P.R. and A.P. Gagge. 1988. "Rationalization of the effective temperature ET*, as a measure of the enthalpy of the human indoor environment." *ASHRAE Transactions* Vol. 94, Part 1, pp. 12-31.

3. ASHRAE. 1981. *ANSI/ASHRAE Standard 55-1981*, "Thermal environmental conditions for human occupancy." Atlanta: American Society of Heating, Refrigerating, and Air-Conditioning Engineers, Inc.

4. Harris, Louis and Associates. 1980. *The Steelcase national study of office environments, No. II. Comfort and productivity in the office of the 80's.* Grand Rapids, MI: Steelcase, Inc.

5. Brill, M. 1984. *Using office design to increase productivity.* Buffalo, N.Y.: Workplace Design and Productivity, Inc.

6. Woods, J., G. Drewry, and P. Morey. 1987. "Office worker perceptions of indoor air quality effects on discomfort and performance." Proceedings: *4th International Conference on Indoor Air Quality and Climate*, 17-21 August, Berlin, pp.464-68. Berlin: Institute for Water, Soil, and Air Hygiene.

7. Dillon, R., and J.C. Vischer. 1987. *Derivation of the tenant questionnaire survey assessment method: Office building occupant survey data analysis.* Public Works Canada, AES/SAG 1-4:87-9.

8. Baillie, A.P., I.D. Griffiths, and J.W. Huber. 1987. *Thermal comfort assessment: A new approach to comfort criteria in buildings.* Department of Psychology, University of Surrey, Guildford, UK, Final Report ETSU S-1177.

9. Schiller, G.E., E.A. Arens, F.S. Bauman, C.C. Benton, M. Fountain, and T. Doherty. 1988. "A field study of thermal environments and comfort in office buildings." *ASHRAE Transactions*, Vol. 94, Part 2.

10. ISO. 1984. *International Standard 7730*, "Moderate thermal environments -- determination of the PMV and PPD indices and specification of the conditions for thermal comfort." Geneva: International Standards Organization.

11. Croome, D.J., and D. Rollason. 1988. "Freshness, ventilation and temperature in offices." *Proceedings of CIB Conference Healthy Buildings 88*, 5-8 September, Stockholm.

12. Harris, L., and Associates. 1989. *Office environment index 1989*. Grand Rapids, MI: Steelcase, Inc.

13. Hart, G.H., and D. Int-Hout III. 1981. "The performance of a continuous linear diffuser in the interior zone of an open office environment." *ASHRAE Transactions*, Vol. 87, Part 2.

14. Public Works Canada. 1983. "Harry Hays Building, Calgary, Alberta -- Stage 1 in the Development of Total Building Performance -- Volume 9: Air Circulation." Public Works Canada, Architectural and Building Sciences, September.

15. Tilley, B. 1988. "Air Circulation Evaluation." Ottawa, Ontario: Architectural & Engineering Services, Public Works Canada, Document D09, March.

16. Huvinen, T., and M. Rantama. 1987. "Individual air conditioning control at open plan offices." Proceedings: *ROOMVENT-87, Air Distribution in Ventilated Spaces*, 10-12 June, Stockholm.

17. Nguyen, V.H. 1990. "Ventilation effectiveness of different diffusers with partitions." Proceedings: *ROOMVENT-90,* Second International Conference, 13-15 June, Oslo.

18. Bauman, F.S., and E.A. Arens. 1988. "The development of a controlled environment chamber for the physical and subjective assessment of human comfort in office buildings." In: *A New Frontier: Environments for Innovation, Proceedings: International Symposium on Advanced Comfort Systems for the Work Environment*, W. Kroner, ed. Troy, N.Y.: Center for Architectural Research.

19. Benton, C.C., F.S. Bauman, and M.E. Fountain. 1990. "A field measurement system for the study of thermal comfort." *ASHRAE Transactions*, Vol. 96, Part 1.

20. Sandberg, M. And M. Sjoberg. 1983. "The use of moments for assessing air quality in ventilated rooms." *Building and Environment*, Vol. 18, pp. 181-197.

21. Fisk, W.J., R.J. Prill, and O. Seppanen. 1988. "Commercial building ventilation measurements using multiple tracer gases." Proceedings: *9th AIVC Conference, Effective Ventilation*, Vol. 1, pp. 161-182. Coventry, Great Britain: Air Infiltration and Ventilation Centre.

22. Fisk, W.J., R.J. Prill, and O. Seppanen. 1989. "A multi-tracer technique for studying rates of ventilation, air distribution patterns, and air exchange efficiencies." Proceedings: *Building systems: Room air and air contaminant distribution*, pp. 237-240. Atlanta: American Society of Heating, Refrigerating, and Air-Conditioning Engineers, Inc.

23. Haarje, D. 1990. Personal Communication. Princeton University, Princeton, NJ.

24. Fisk, W.J. et al. 1985. "Multi-tracer system for measuring ventilation rates and ventilation efficiencies in large mechanically ventilated buildings." In Supplement to Proceedings: *6th AIVC Conference, Ventilation Strategies and Measurement Techniques*, pp. 69-93. Coventry, Great Britain: Air Infiltration and Ventilation Centre.

25. Schenck, H. 1979. *Theories of engineering experimentation*, 3rd ed. New York: McGraw-Hill.

LIST OF TABLES AND FIGURES

Table 1. Thermal Measurement Test Conditions

Test Number	Supply Air Volume (cfm)	Heat Load (W/sq.m)	Return Air Volume (cfm)	Supply Air Temp. (deg C)	Room Temp* (deg C)	Return Air Temp. (deg C)	Partition Height (inches)	Partition Air Gap	Diffuser Location**
P1A	55	55	-	16.5	27.9	-	65	Solid	(5,2)
P1B	54	55	-	16.7	28.5	-	65	Open	(5,2)
P2A	108	35	-	12.8	23.9	-	65	Solid	(5,4)
P2B	107	35	-	13.0	23.8	-	65	Open	(5,4)
P3A	179	55	-	13.9	25.1	-	65	Solid	(5,2)
P3B	180	55	-	14.3	25.8	-	65	Open	(5,2)
1A	152	55	133	13.1	24.2	24.3	65	Solid	(5,2)
1B	152	55	133	13.0	24.2	24.4	65	Open	(5,2)
2A	154	55	143	13.0	24.5	24.7	65	Two inch	(5,2)
2B	154	55	144	13.1	24.1	24.6	65	Solid	(5,2)
3A	157	55	144	18.0	26.4	26.5	65	Solid	(5,2)
3B	152	55	157	18.0	26.0	26.5	65	Open	(5,2)
4A	155	35	133	13.2	21.9	21.6	65	Open	(5,2)
4B	154	35	114	13.3	22.1	21.5	65	Solid	(5,2)
5A	319	55	258	15.5	23.6	23.5	65	Solid	(5,2)
5B	319	55	260	13.3	23.2	23.0	65	Open	(5,2)
6A	300	55	200	13.8	22.0	22.6	65	Comb.	(5,2)
6B	305	55	201	13.4	21.9	22.6	65	Two inch	(5,2)
6C	296	55	201	13.3	22.0	22.6	65	Solid	(5,2)
7A	171	55	143	13.3	25.0	25.1	75	Solid	(5,2)
7B	170	55	143	13.0	25.3	25.2	75	Open	(5,2)
7C	170	55	145	13.1	25.4	25.4	65	Solid	(5,2)
8A	288	55	249	18.2	25.0	24.9	75	Open	(5,2)
8B	288	55	249	17.9	25.2	25.2	75	Solid	(5,2)
8C	289	55	252	18.0	25.5	25.5	65	Solid	(5,2)
9A	291	55	246	18.3	24.3	25.0	65	Solid	(5,2)
9B	292	55	241	18.0	24.5	25.1	65	Four inch	(5,2)
9C	293	55	245	18.0	24.9	25.3	75	Four inch	(5,2)
10A	282	55	236	18.1	24.6	24.9	65	Open	(8,5)
10B	282	55	237	17.9	24.7	25.1	65	Solid	(8,5)
11A	290	55	241	18.1	23.5	25.2	65	Open	(2,8)
11B	291	55	241	18.0	23.5	25.2	65	Solid	(2,8)
12A	320	55	255	19.3	24.3	24.9	65	Open	(5,2)
12B	320	55	258	19.5	24.8	25.5	65	Solid	(5,2)
13A	309	55	259	17.9	24.4	24.7	65	Open	(2,2)(8,2)
13B	309	55	259	18.0	24.6	24.9	65	Solid	(2,2)(8,2)
14	312	55	277	17.0	24.6	24.7	None	-	(5,2)
15	308	55	276	16.9	24.5	24.5	42	Solid	(5,2)
16	169	55	160	13.0	23.7	24.3	42	Solid	(5,2)

*Room temperature measured at height of 4.5 ft on chamber wall

**Refer to Figure 3

Table 2. Tracer Gas Test Conditions

Test Number	Supply Air Volume (cfm)	Supply Air Temp (deg C)	Room Temp (deg C)	Partition Height (inches)	Partition Air Gap	Diffuser Location**	Comments
21	100	13	24	65	Solid	(5,4)	
22W	100	15	24	65	Solid	(5,4)	Mixing fans in CEC
22*	100	15	24	65	Solid	(5,4)	
23	150	25	22	65	Solid	(5,4)	Heating test
24	110	14	24	65	S&O+	(5,4)	
25	110	14	26	65	S&O	(5,2)	
39	210	na	24	75?	Solid	(5,2)	
40	200	18	24	75	Open	(5,2)	
41	55	18	26	75	Solid	(5,2)	
42W	100	13	26	65	Open	(5,2)	Mixing fans in CEC
43	100	25	23	75	Solid	(5,2)	Heating test
45	70	25	22	75	Solid	(5,2)	Heating test
46	100	25	23	75	Solid	(5,2)	Heating test

*Tracer decay, all other tests are tracer stepup

** See Figure 3

+Partition gaps open in WS 1&2

Table 3. Air Diffusion Performance Index (ADPI) Results

SAV (cfm/sqm)	Load (w/sqm)	SAT (degC)	Part (in.)	Gap	Test	ADPI
5-6	35	13	65	S	4B	95%
				O	4A	99%
	55	13	42	S	16	94%
			65	S	7C	93%
				O	1B	94%
			75	S	7A	99%
				O	7B	96%
		18	65	S	3A	90%
				O	3B	89%
10-11	55	13-15	65	S	5A	90%
				O	5B	90%
		18	0	-	14	95%
			42	S	15	89%
			65	S	8C	91%
				O	12A	91%
			75	S	8B	90%
				O	8A	98%

Table 4. Air Gap Velocities: Test 12A

Gap Location*	10-in. Gap	8-in. Gap	6-in. Gap	4-in. Gap	2-in. Gap
1	0.27	0.32	0.22	0.36	0.30
2	0.18	–	0.19	0.18	–
3	0.11	–	0.06	0.16	–
4	0.20	0.20	0.23	0.24	0.18
5	0.08	–	0.16	0.11	–
6	0.15	–	0.15	0.16	–
7	0.07	–	0.11	0.07	–

*See Figure 15

Table 5. Comfort Model Results
(RH = 50%, 0.5 clo, 1.2 met)

Test No.	WS No.	ET* (deg C)	DISC	PMV
11A	1	26.4	0.55	0.56
	2	26.1	0.48	0.50
	3	25.8	0.40	0.41
11B	1	25.9	0.41	0.43
	2	25.9	0.41	0.43
	3	25.7	0.39	0.39
12A	1	26.6	0.60	0.61
	2	27.2	0.77	0.77
	3	25.5	0.33	0.33
12B	1	26.5	0.59	0.60
	2	27.1	0.70	0.75
	3	25.6	0.36	0.36
14	1	25.4	0.32	0.31
	2	25.4	0.31	0.31
	3	25.4	0.31	0.31
15	1	26.3	0.53	0.54
	2	26.7	0.60	0.63
	3	25.3	0.28	0.28
16	1	24.0	0.00	-0.02
	2	25.6	0.33	0.35
	3	24.5	0.08	0.08

Table 6. Age of Air Measurements (in hours):
Based on data from Well-Mixed Tests No. 22W and 42W

Sample point	Age of Air Test 22W	Test 42W
1C	0.41	0.55
1B·	0.45*	0.52
1K	0.45	0.51
2C	0.44	0.57
2B	0.43*	0.52
2K	na	0.51
3C	0.46*	0.50
3B	0.45*	0.49
3K	0.47	0.46
4C	0.44	0.49
4B1	0.43	0.48
4B2	0.44*	0.49
4K	0.45	0.51
5B	0.44	0.54
6C	0.43	0.51
6B	0.43	0.53
7B	0.44	0.49
8C	0.46	0.48
Return duct	0.45	0.51
Average	0.440	0.510
Std. Dev.	0.010	0.030
Coeff. of Var.	3.1%	5.3%

Numbers correspond to locations in Figure 6
C: Ceiling level (2.1m above floor)
B: Breathing Level (1.1m above floor)
K: Knee Level (0.4m above floor)
* Age computed by numerical integration

Table 7. Averages of Local Ages of Air (in Hours) for Different Heights

Test Number	Knee (0.4m)	Breathing (1.1m)	Ceiling (2.1m)	Return
21	0.45	0.40	0.39	0.43
22W	0.46	0.44	0.44	0.45
22	0.40	0.39	0.40	0.44
23	0.35	0.38	0.32	0.28
24	0.43	0.41	0.44	0.43
25	0.45	0.39	0.43	0.44
39	0.27	0.27	0.27	0.30
40	0.25	0.26	0.27	0.29
41	0.79	0.78	0.86	0.88
42W	0.50	0.50	0.52	0.51
43	0.50	0.53	0.48	0.49
45	0.84	0.87	0.84	0.78
46	0.58	0.63	0.57	na

Table 8. Age of Air Ratios Related to Short-circuiting

Test Number	Return	WS Ceiling	Aisle Ceiling
	All WS	All WS	Aisle Breathing
21	1.03	0.93	0.98
22W	1.01	1.00	1.01
22	1.13	1.03	0.98
23*	0.78	0.89	0.79
24	1.02	1.05	1.00
25	1.06	1.05	0.96
39	1.08	1.00	0.99
40	1.14	1.04	0.90
41	1.12	1.09	0.93
42W	1.03	1.04	0.95
43*	0.96	0.92	1.03
45*	0.91	0.98	1.00
46*	na	0.95	na

Return: Age in return duct

All WS: Average age of all breathing level (1.1m above floor) and knee level (0.4m above the floor) points in the workstations

WS Ceiling: Average age of all ceiling level (2.1m above floor) points above the workstations

Aisle Ceiling: Location 6 in Figure 6, 2.1m above floor

*Heating test

Table 9. Averages of local ages of air (in hours) for each workstation and the aisle

Test Number	WS 1*	WS 2*	WS 3*	Aisle**
21	0.38	0.47	0.42	0.45
22W	0.45	0.43	0.45	0.44
22	0.38	0.39	0.39	0.42
23	0.35	0.35	0.37	0.38
24	0.41	0.42	0.43	0.44
25	0.39	0.44	0.41	0.55
39	0.28	0.30	0.26	0.30
40	0.25	0.28	0.25	0.30
41	0.74	0.83	0.79	0.89
42W	0.52	0.52	0.49	0.52
43	0.53	0.55	0.49	0.50
45	0.89	0.94	0.80	0.81
46	na	0.64	0.58	0.58

*Averages for WS are for breathing level (1.1m above floor) and knee level (0.4m above floor)

**Averages for aisle are for the breathing level

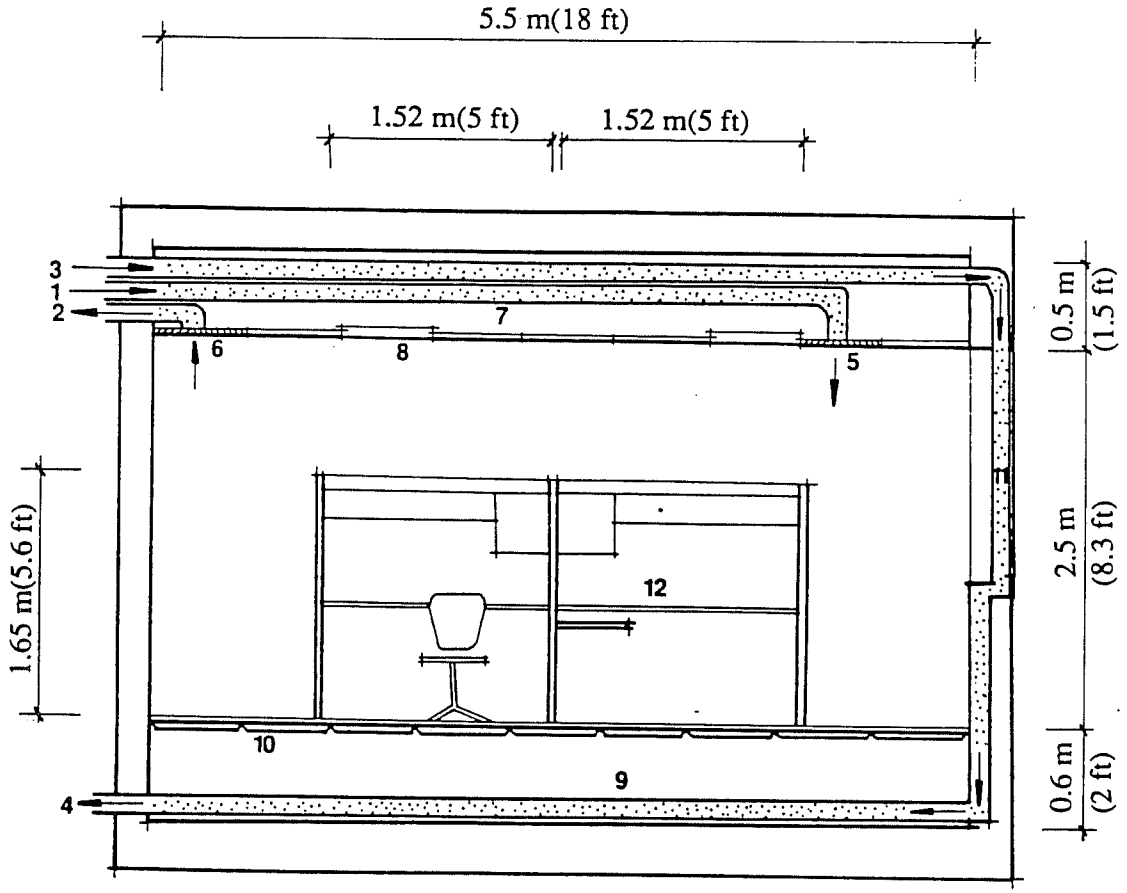

1 ceiling supply
2 ceiling return
3 annular space supply
4 annular space return
5 ceiling supply diffuser
6 ceiling return register
7 ceiling plenum
8 ceiling luminaire
9 sub-floor plenum
10 access floor system
11 window plenum
12 workstation furniture

Figure 1a. Section: Controlled Environment Chamber

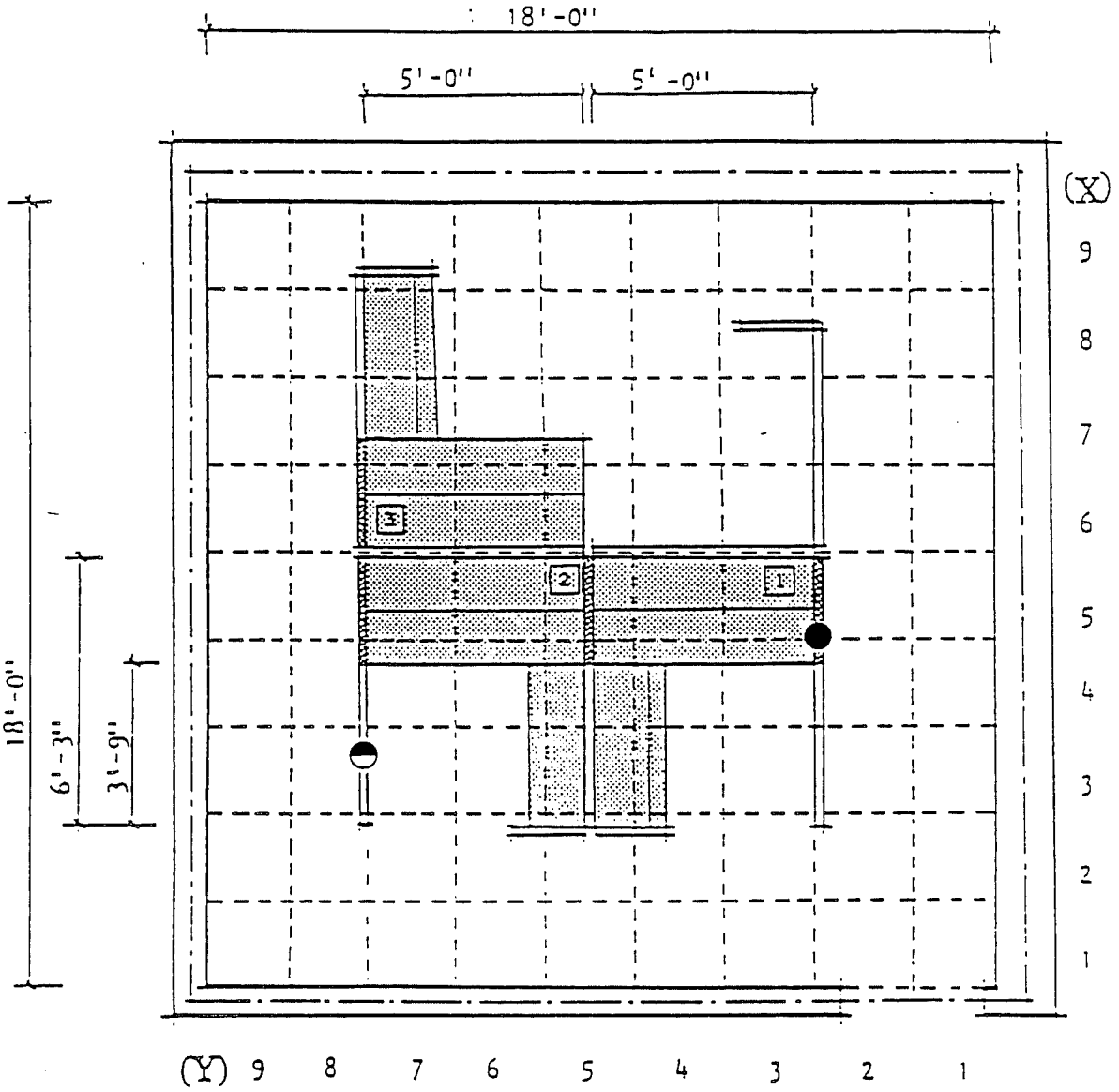

Figure 2a. Test Configuration

● Solid Partition
◒ Airflow/Solid Partition

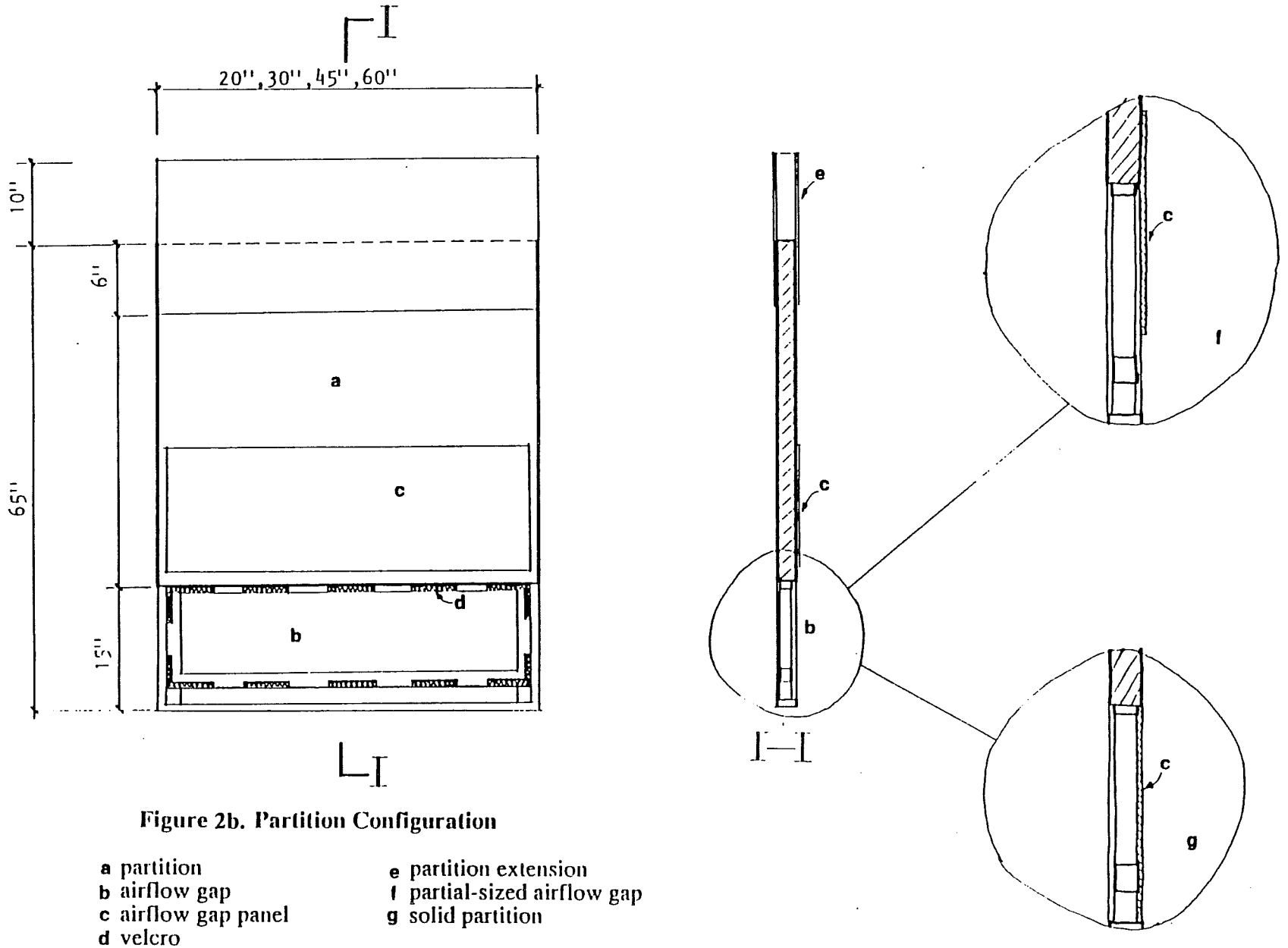

Figure 2b. Partition Configuration

a partition
b airflow gap
c airflow gap panel
d velcro
e partition extension
f partial-sized airflow gap
g solid partition

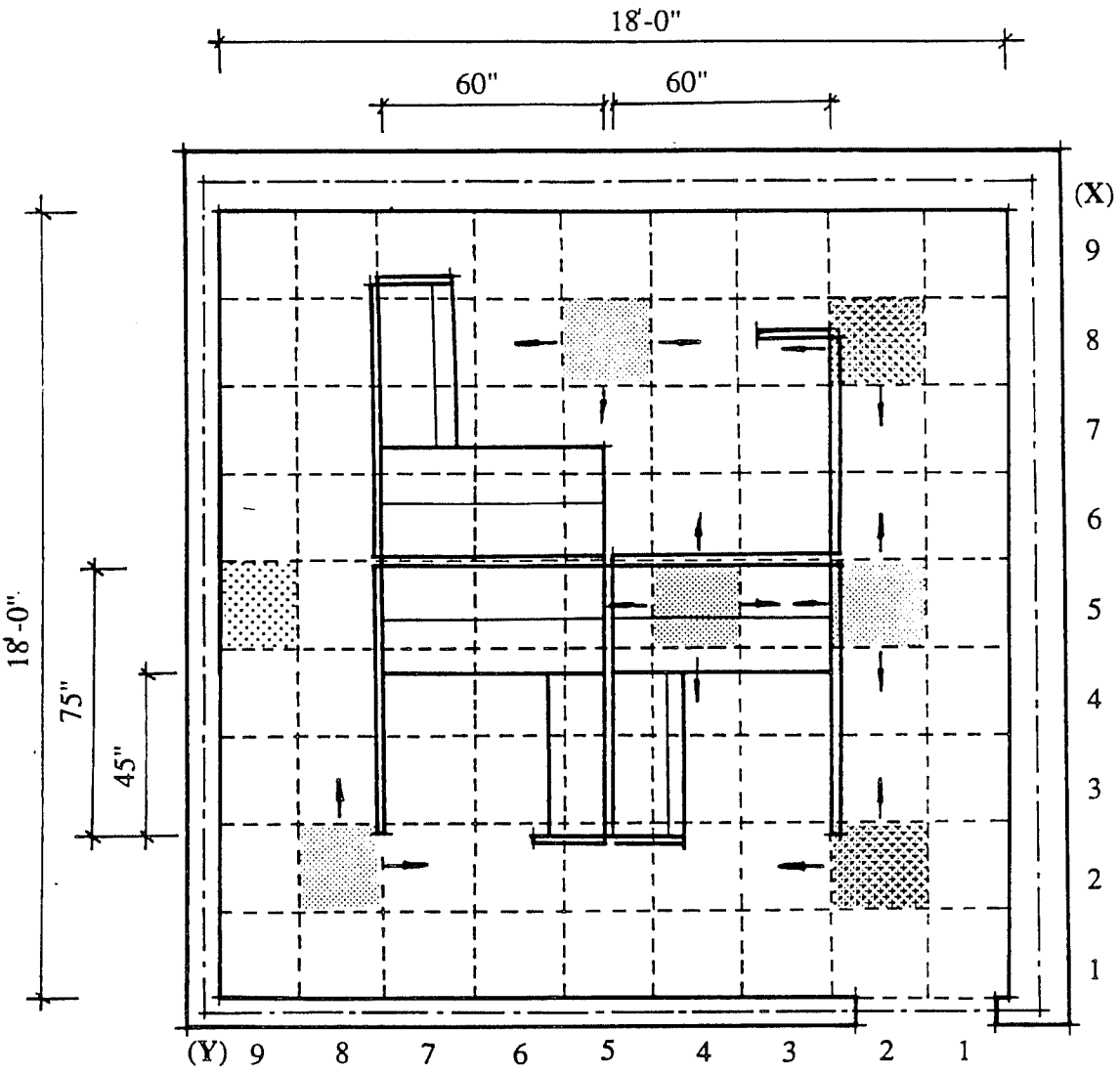

Figure 3. Supply and Return Locations

Return Register
Single Supply Diffuser
Double Supply Diffuser

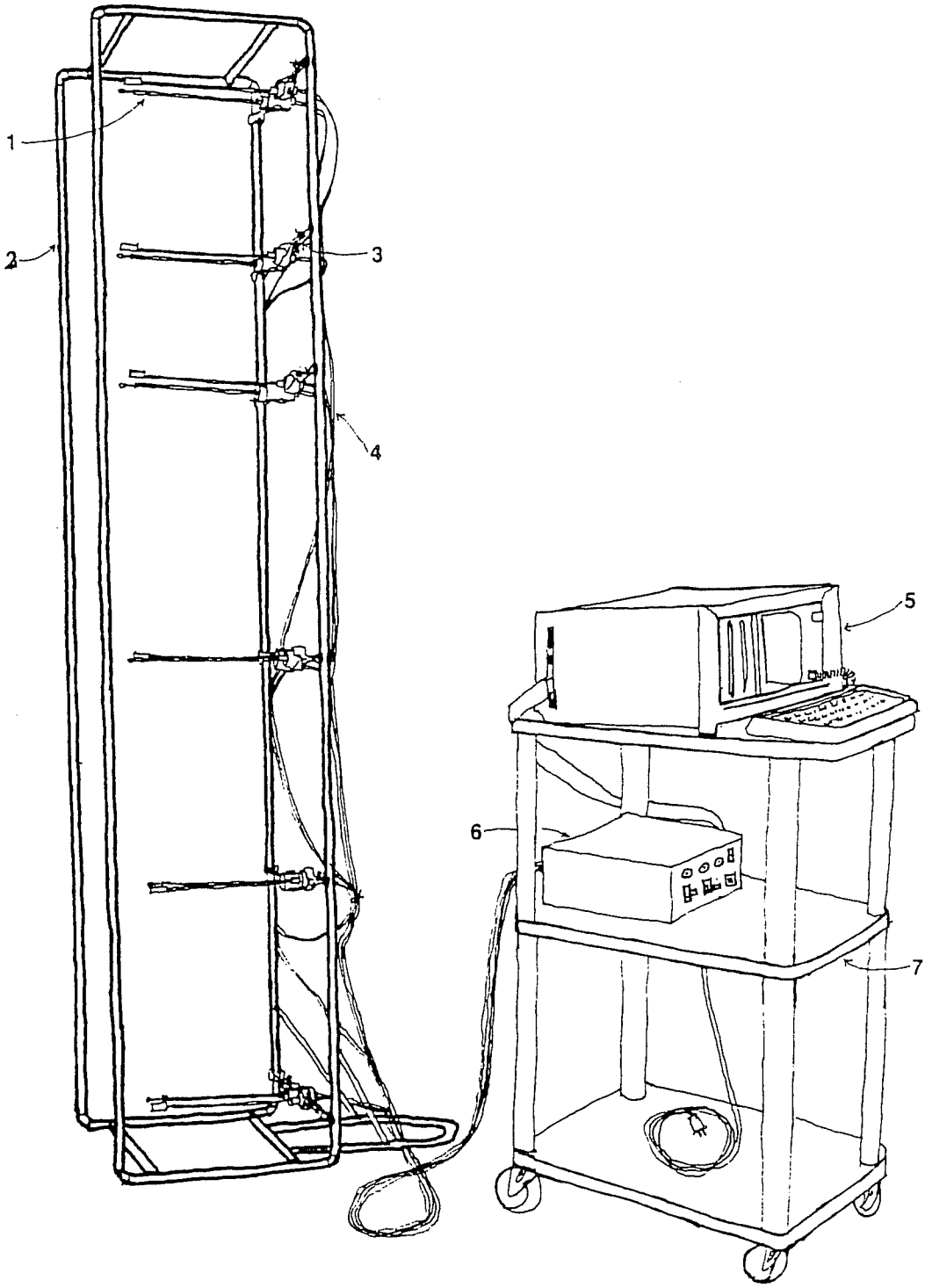

1 anemometers and temperature probes at 0.1m, 0.6m, 1.1m, 1.7m, 2.0m, 2.35m heights
2 sensor rig
3 clamp
4 sensor cable
5 portable computer
6 signal conditioner
7 equipment cart

Figure 4. Sensor Rig and Data Acquisition System

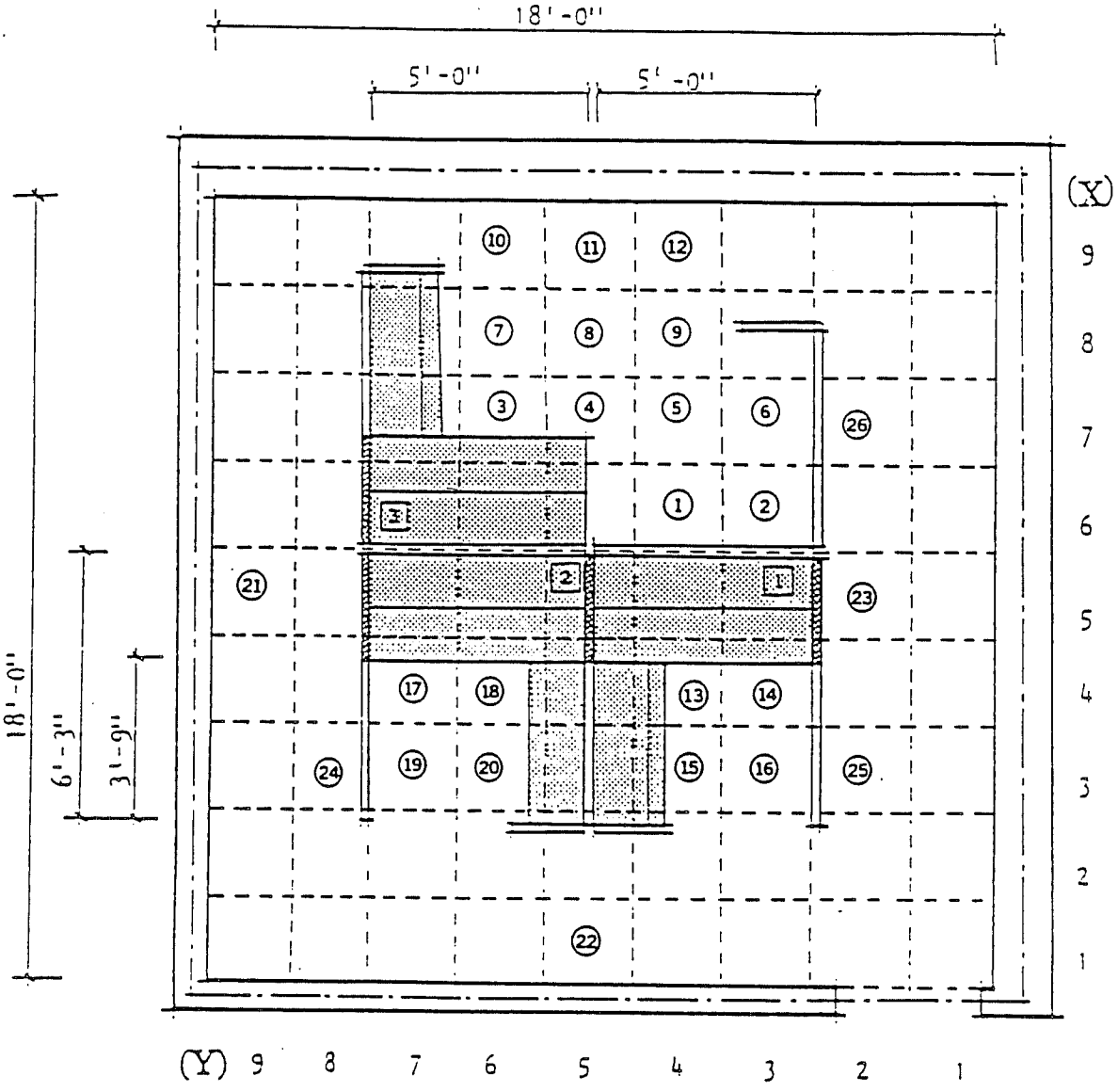

Figure 5. Thermal Measurement Locations

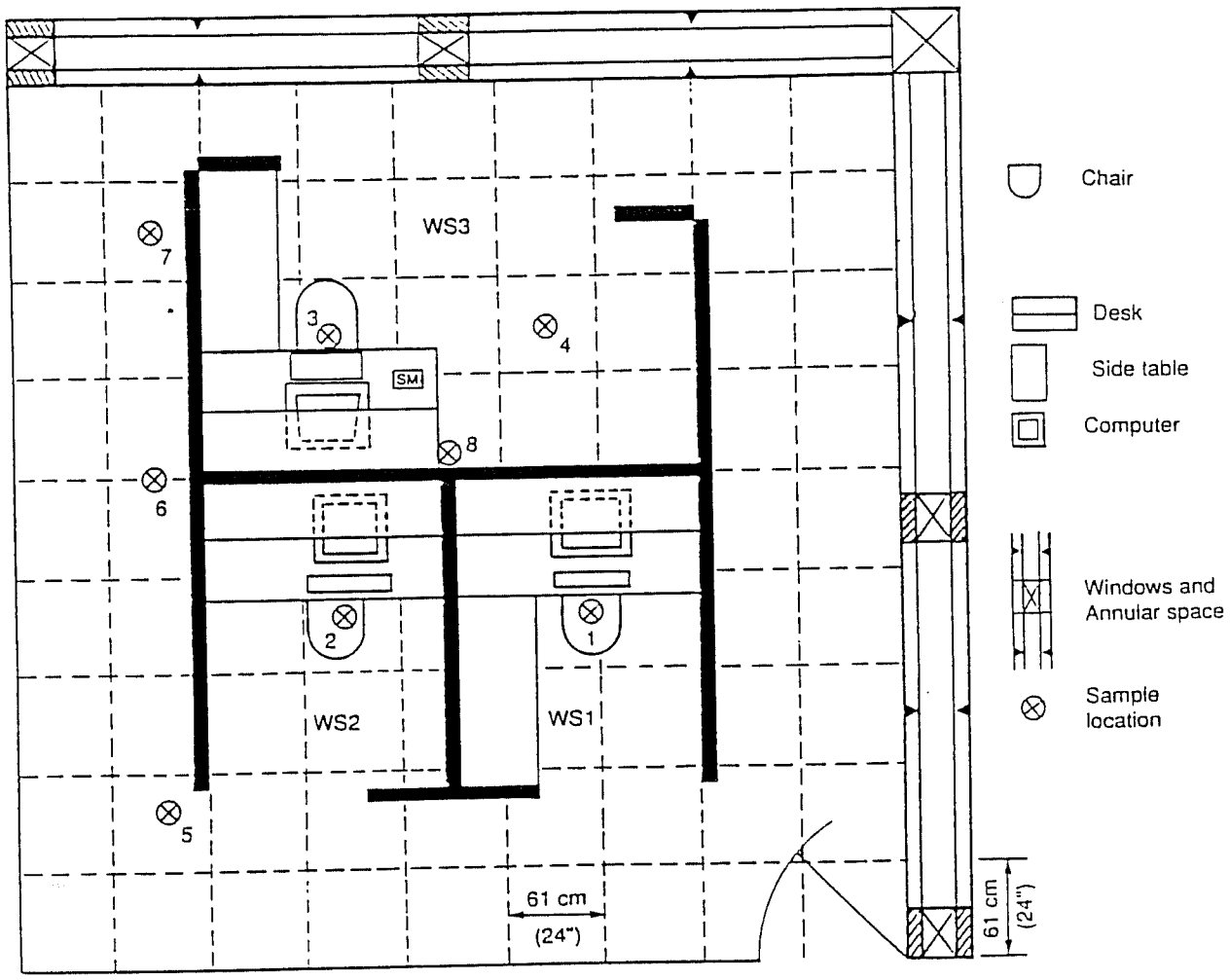

Figure 6. Tracer Gas Sampling Locations

Plan view of CEC with workstations denoted WS1, WS2, WS3. Tracer gas was sampled at points 1-4 (0.4 m, 1.1 m, and 2.1 m above floor), at points 5 & 7 (1.1 m above floor), at point 6 (1.1 m above floor and 2.1 m above floor), and at point 8 (2.1 m above floor).

WS #1

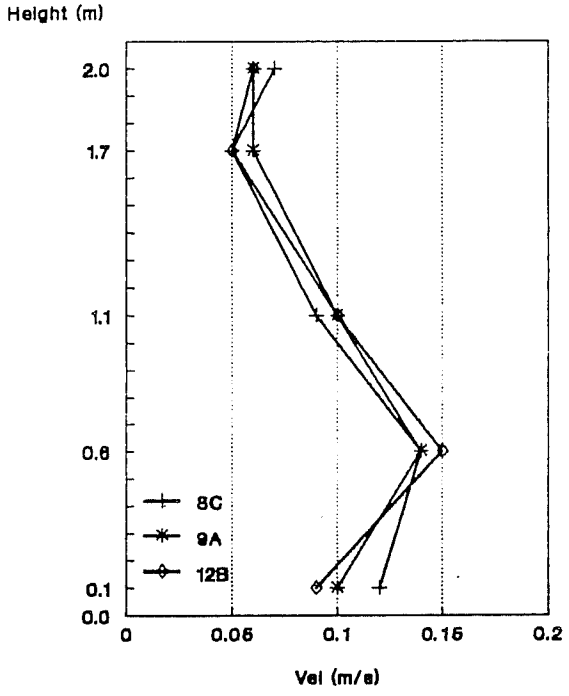

Figure 7A. Repeatability results: Tests: 8C, 9A, 12B

WS #2

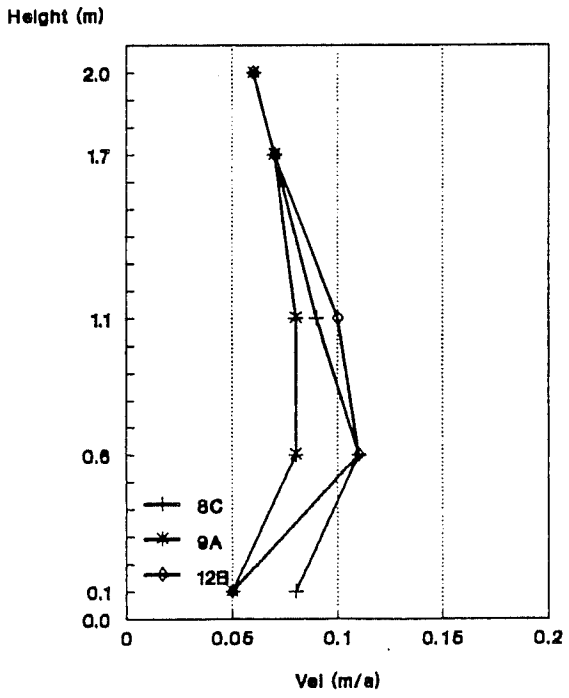

WS #3

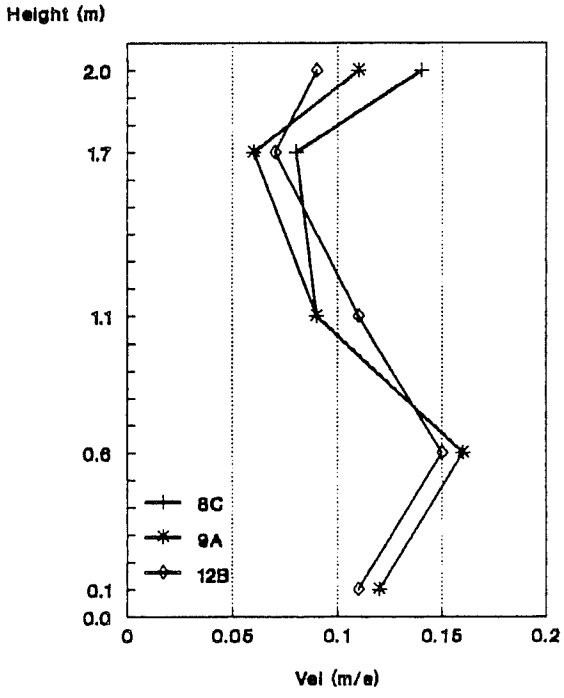

WS #1

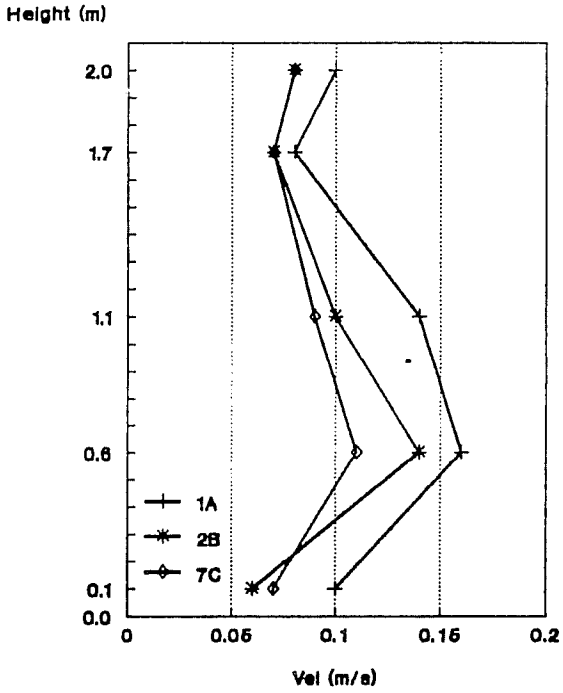

Figure 7B.

Repeatability results:

Tests: 1A, 2B, 7C

WS #2

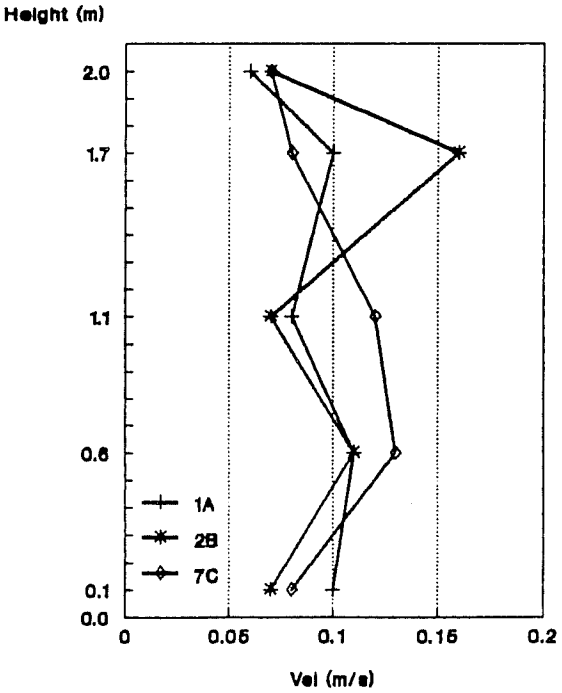

WS #3

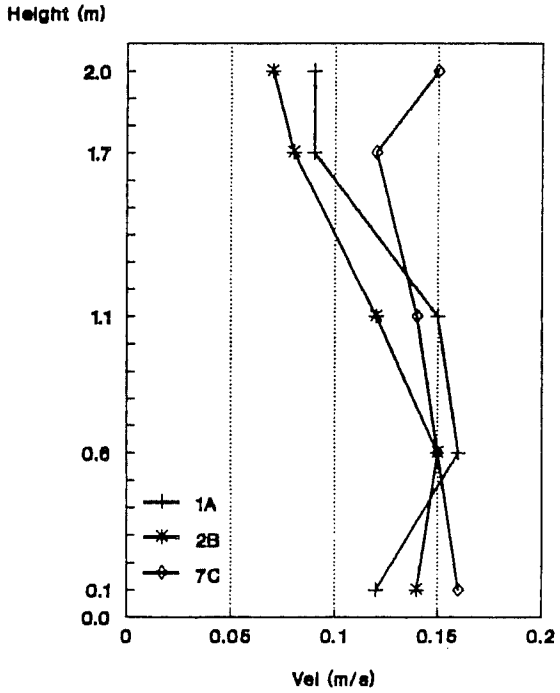

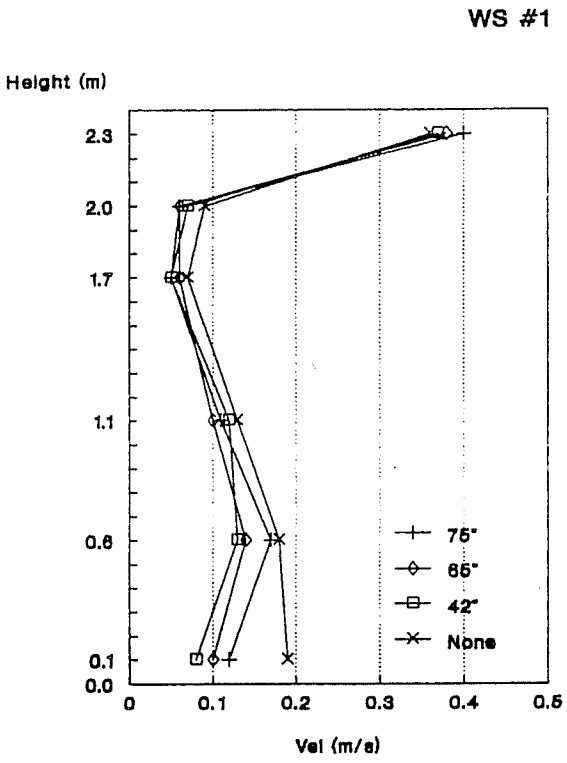

Figure 8A. Solid partition height: Velocity effects

Tests: 8B, 9A, 15, 14

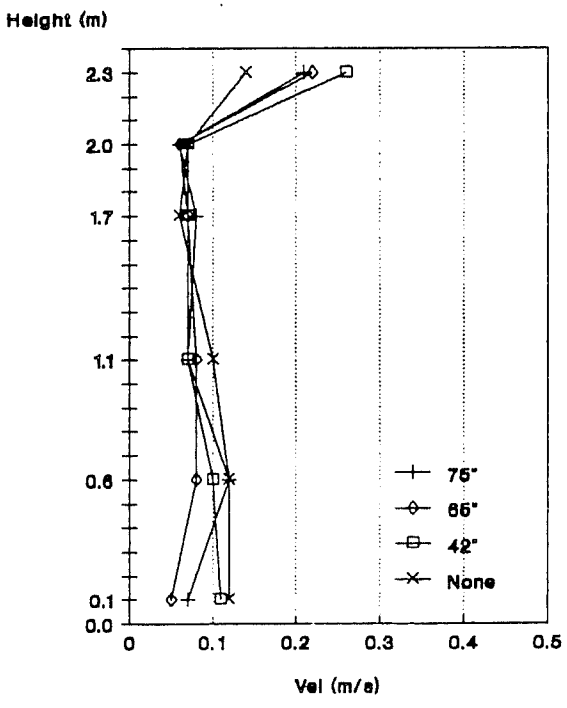

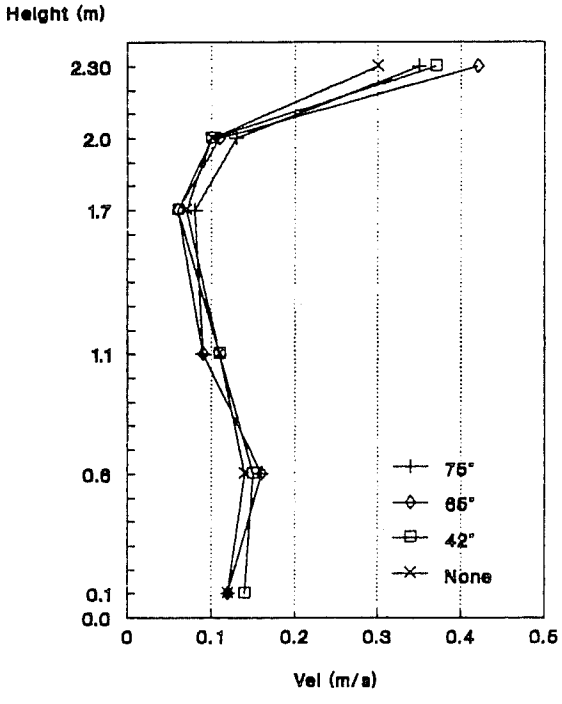

WS #1

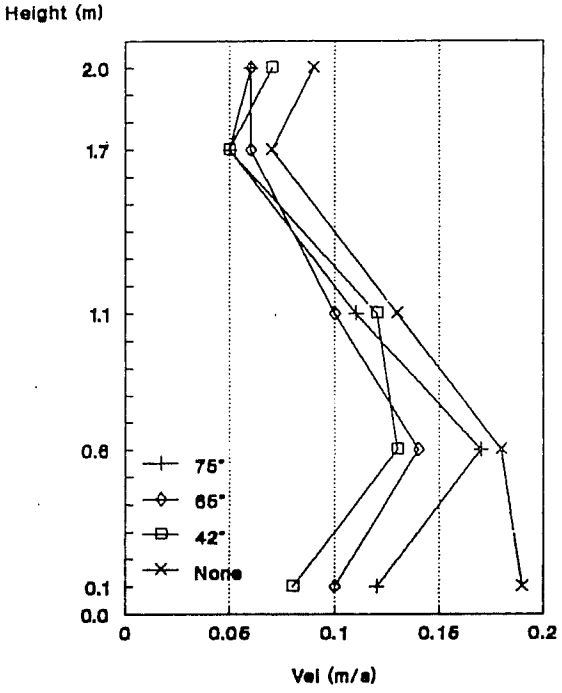

Figure 8B.
Solid partition height:
Velocity effects

Tests: 8B, 9A, 15, 14

WS #2

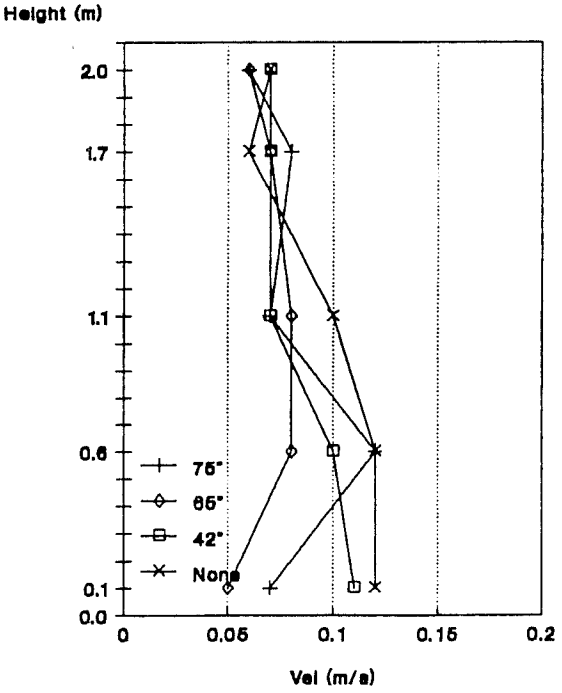

WS #3

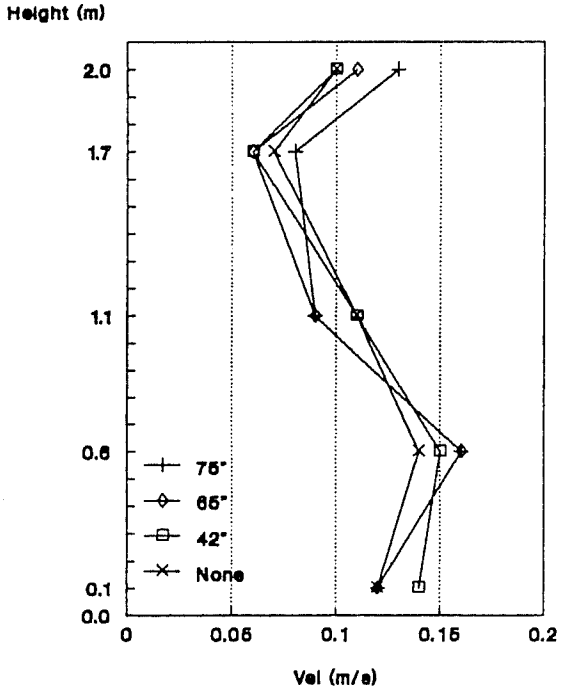

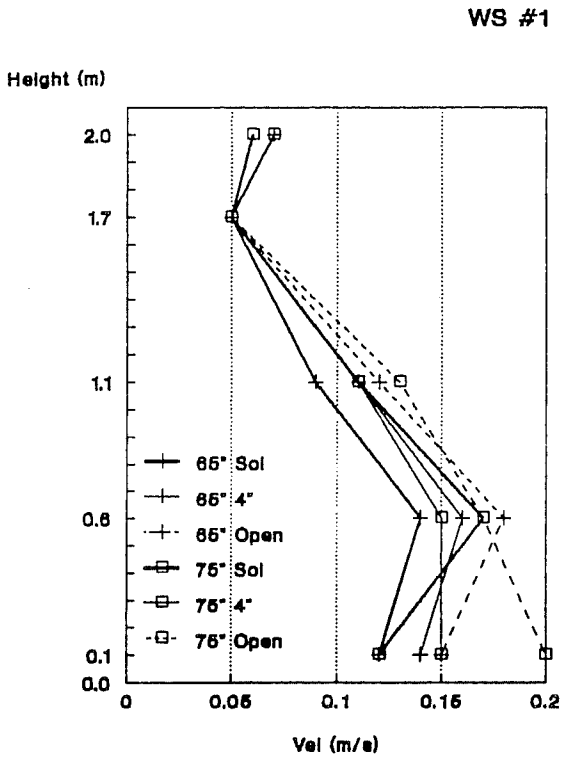

Figure 9. Partition height and gap size: velocity effects

Tests: 8C, 9B, 12A, 8B, 9C, 8A

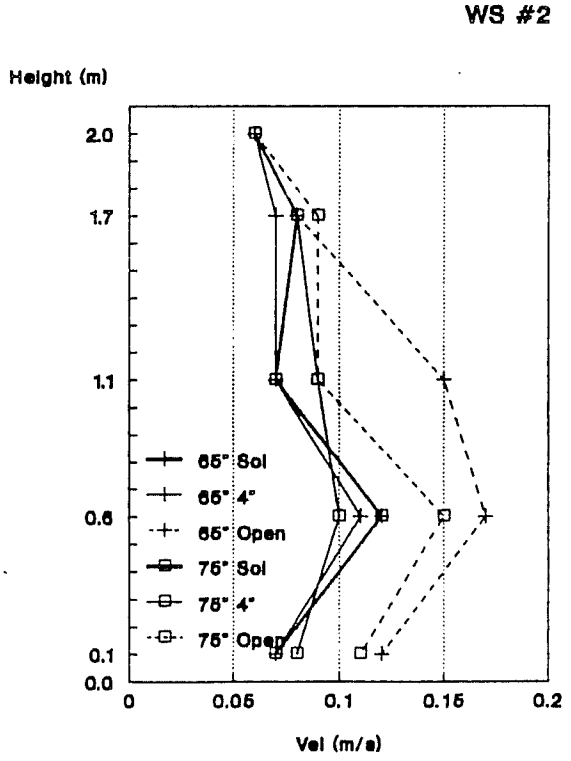

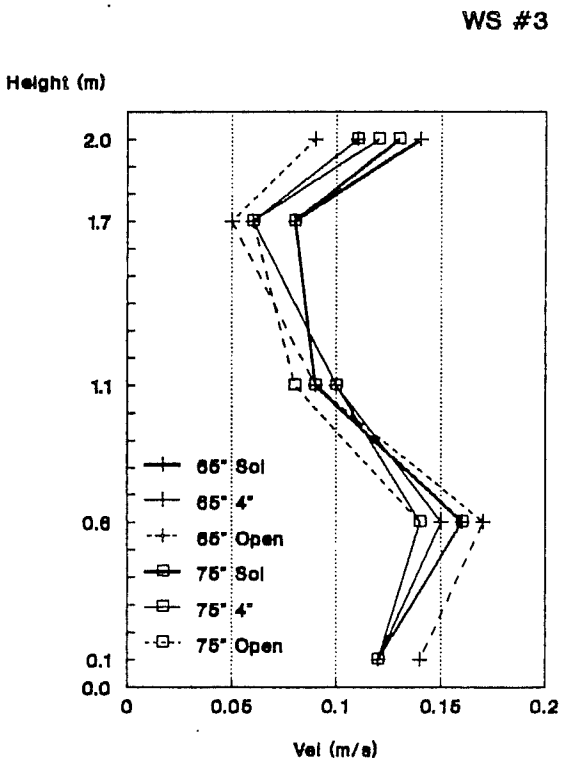

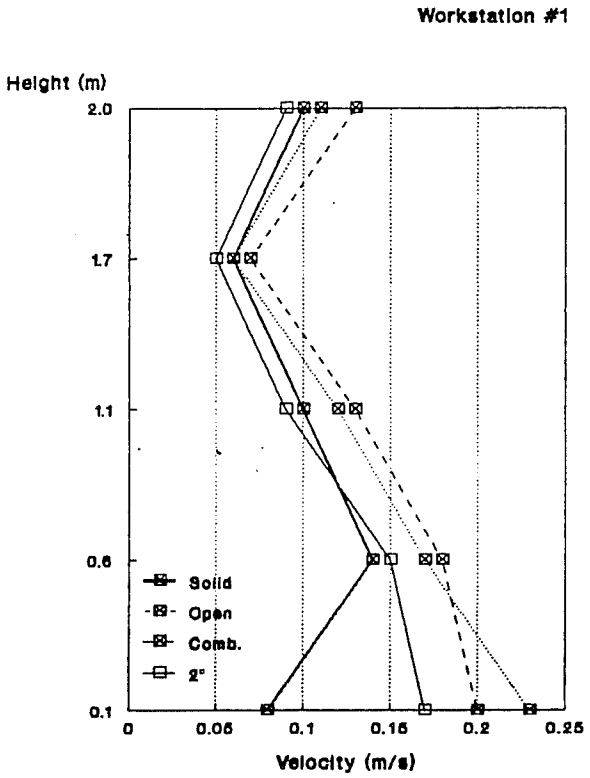

FIGURE 10A

Partition air gap: Velocity effects by workstation

Tests: 5A, 5B, 6A, 6C

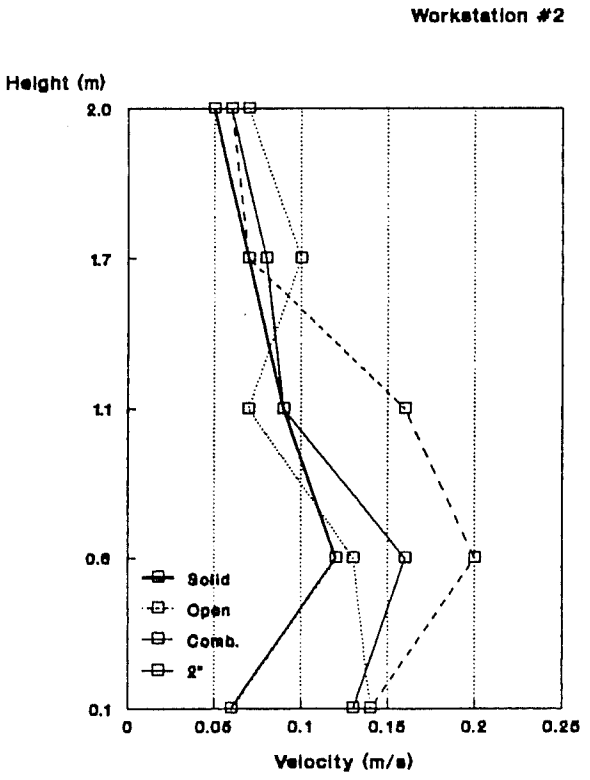

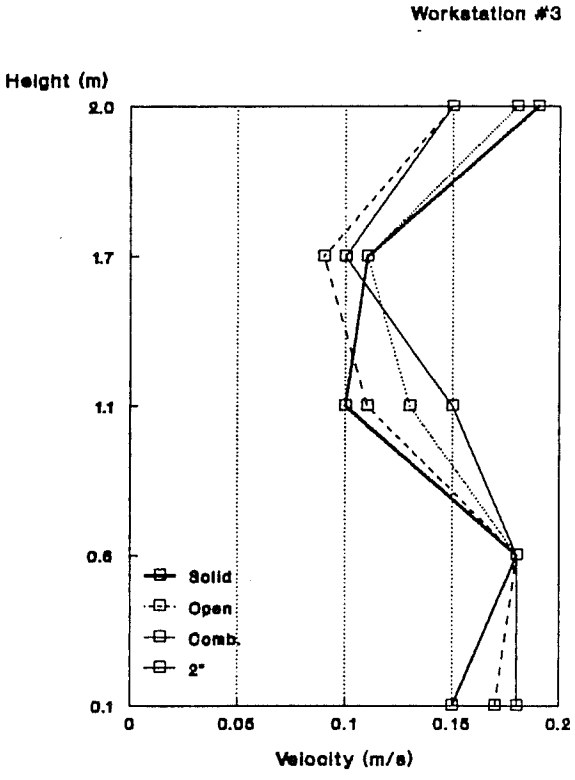

FIGURE 10B Partition air gap: Velocity effects by gap size

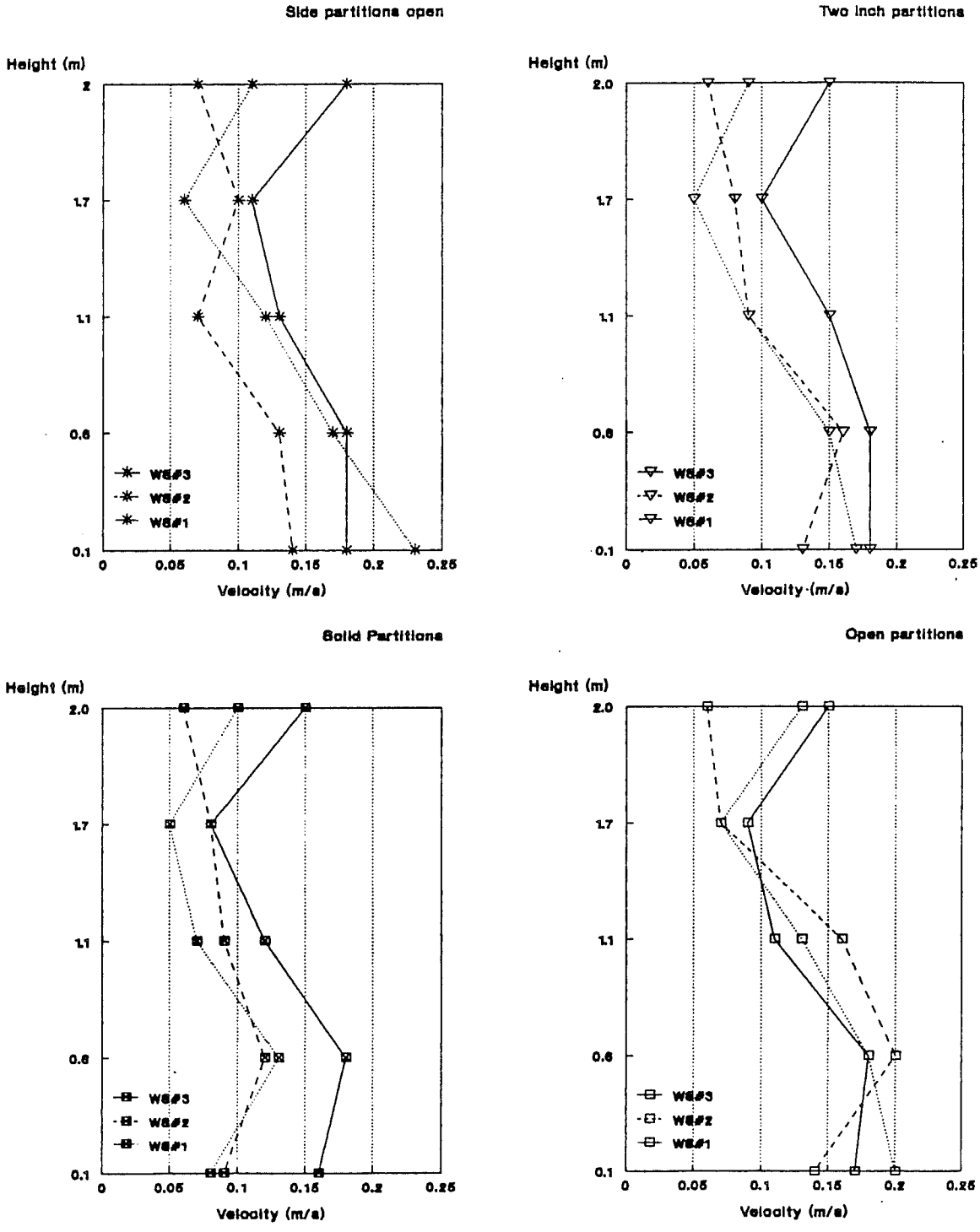

Workstation #1

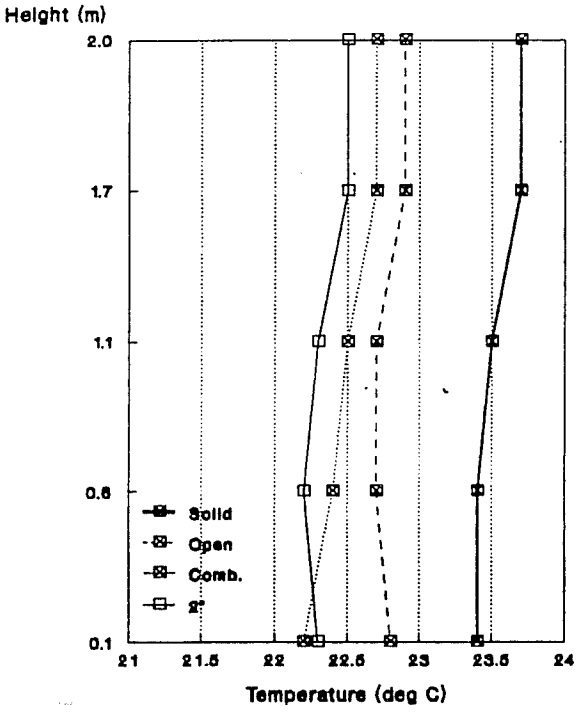

Figure 10C. Partition air gap: Temperature effects

Tests #5A & B, #6A & B

Workstation #2

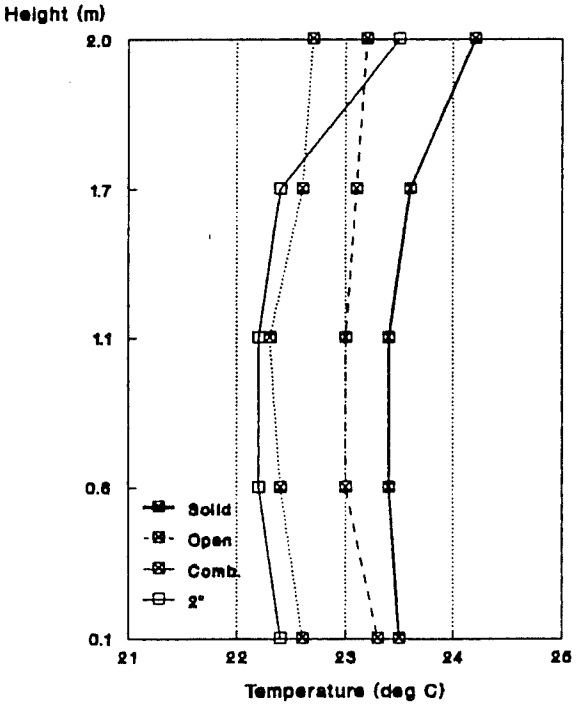

Workstation #3

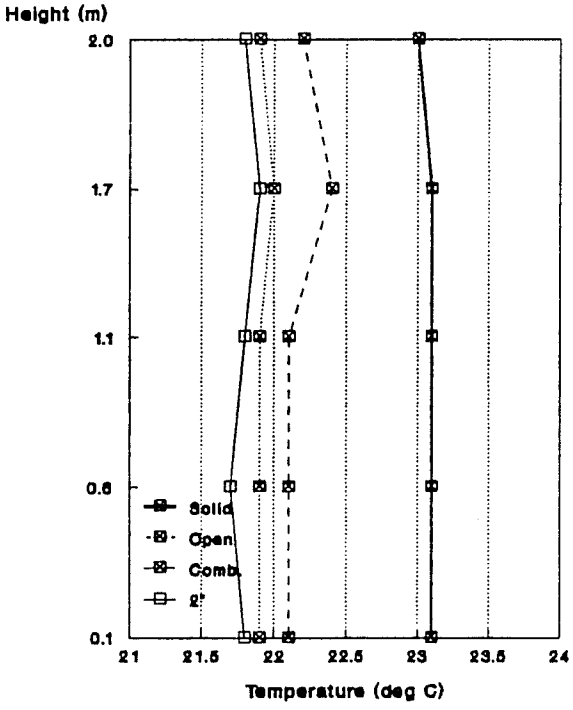

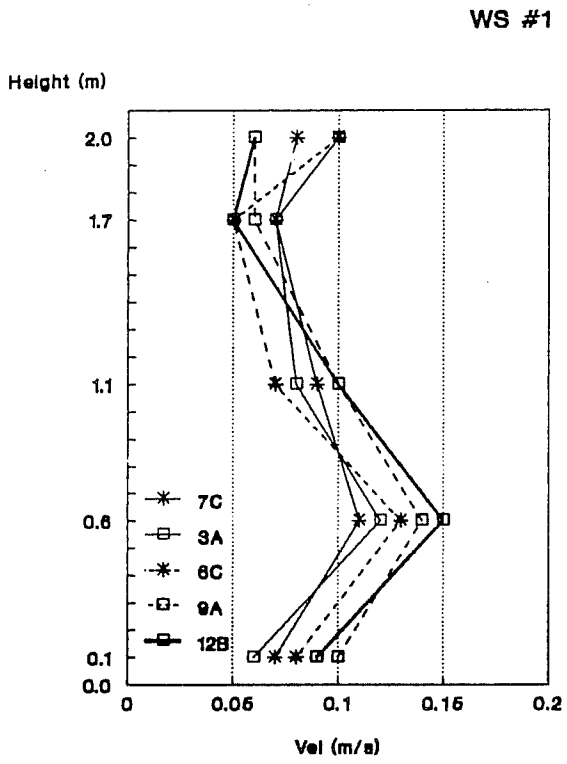

Figure 11A.
Supply air volume and temperature: Velocity effects for solid partitions

Tests: 7C, 3A, 6C, 9A, 12B

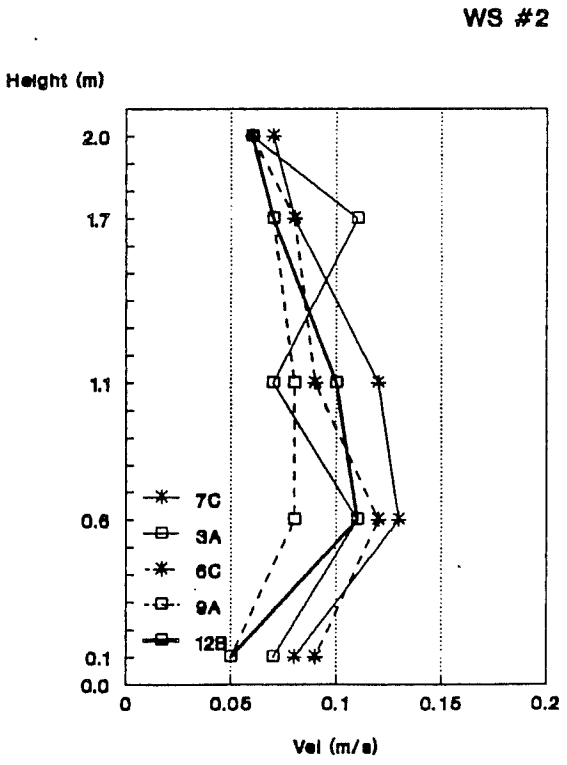

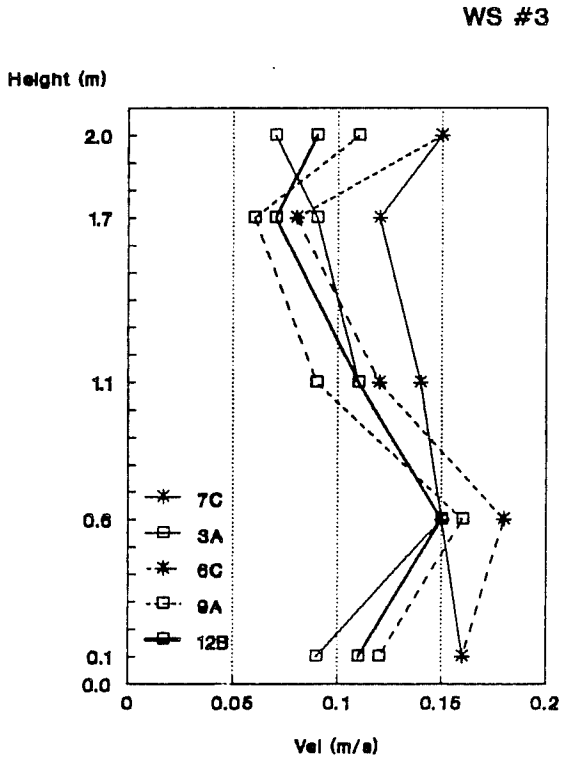

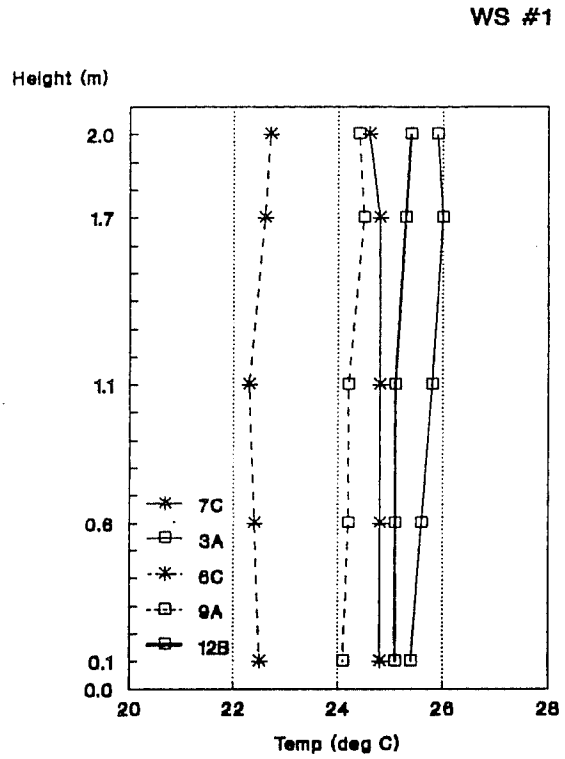

Figure 11B.
Supply air volume and temperature: temperature effects for solid partitions

Tests: 7C, 3A, 6C, 9A, 12B

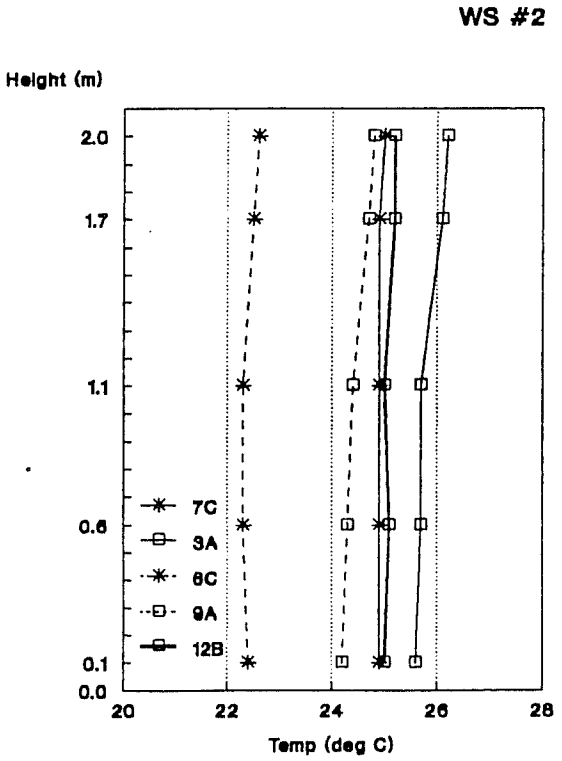

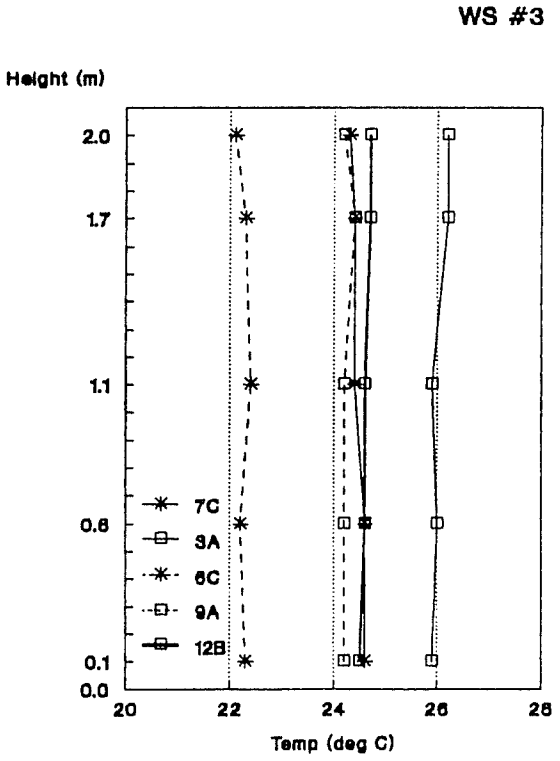

Figure 12A Partition gap size and supply air volume: Velocity effects in WS#1

Tests: 1A, 1B, 2A, 5A, 5B, 6A, 6B

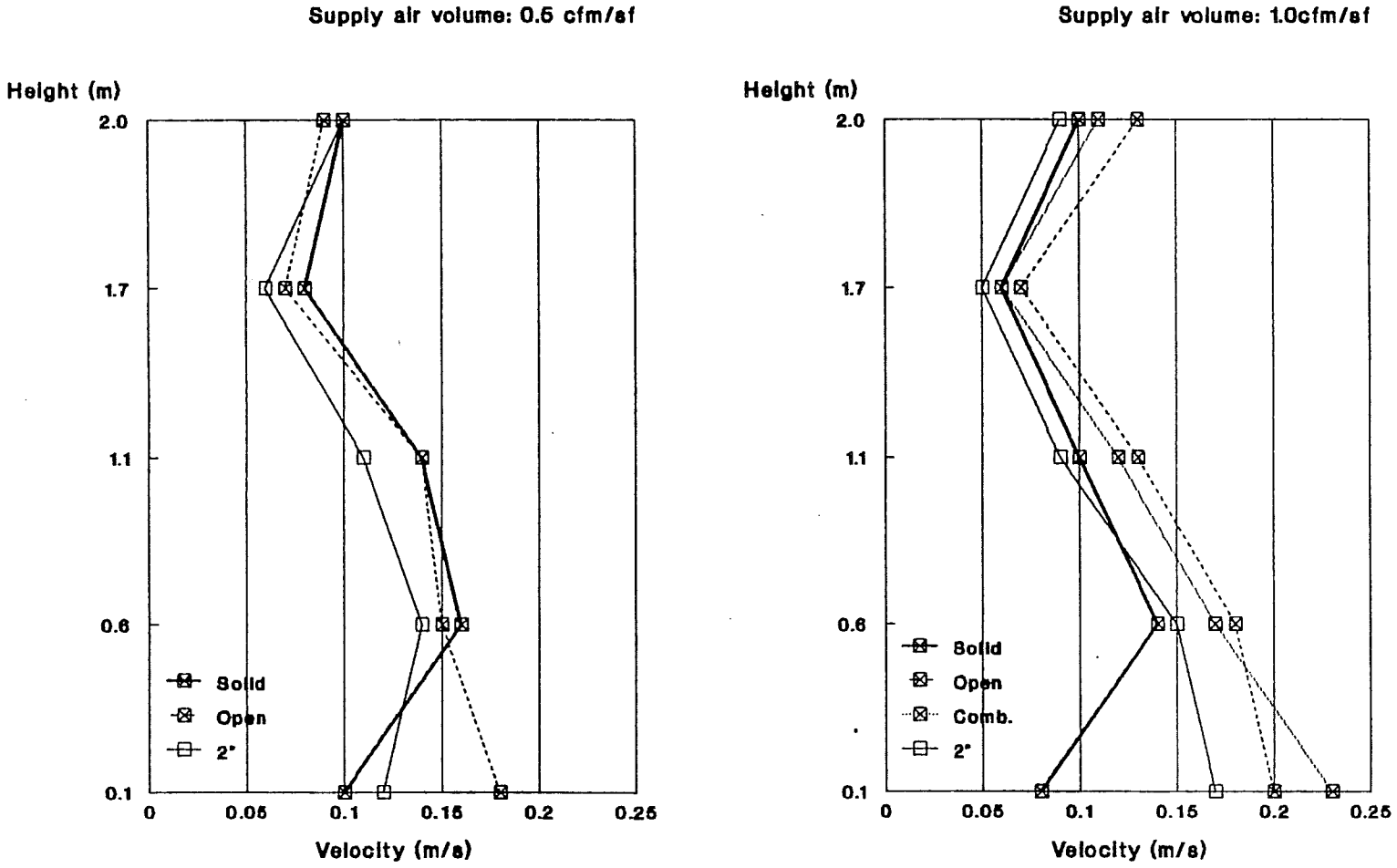

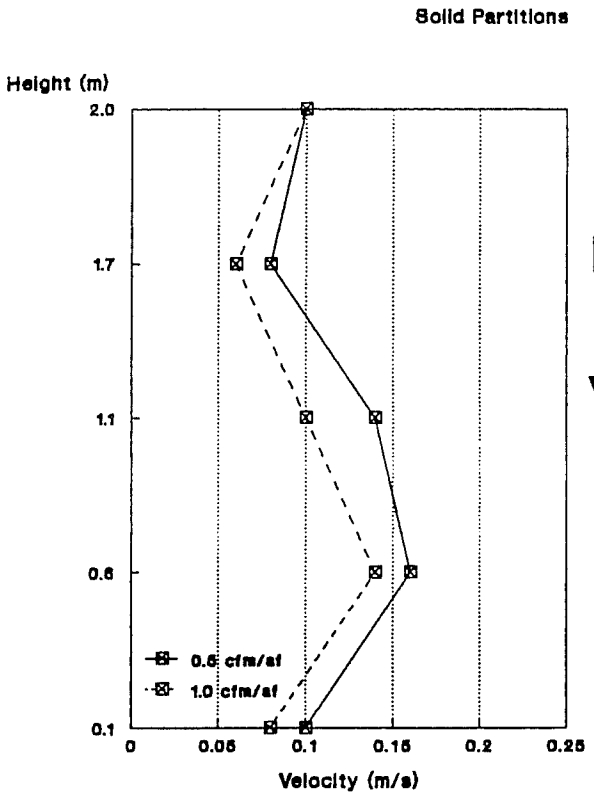

Figure 12B

Partition gap size and supply air volume: Velocity effects in WS#1

Tests: 1A 1B, 5A, 5B 2A, 6B

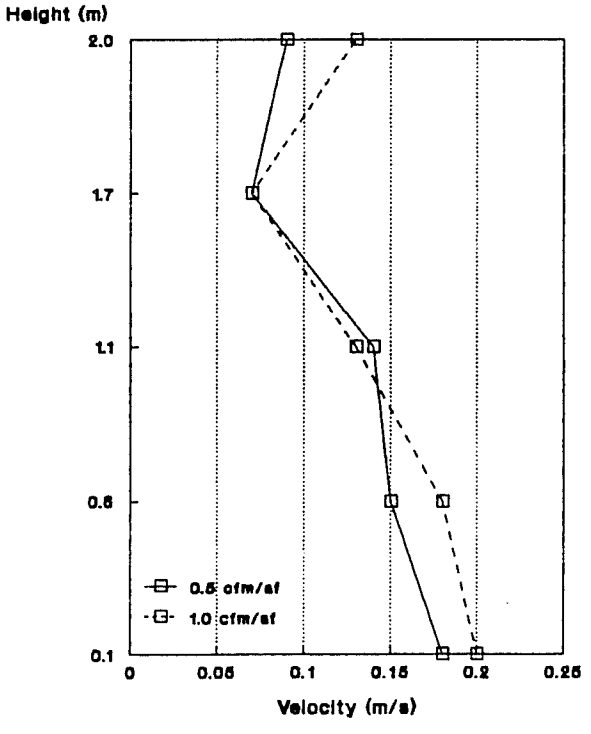

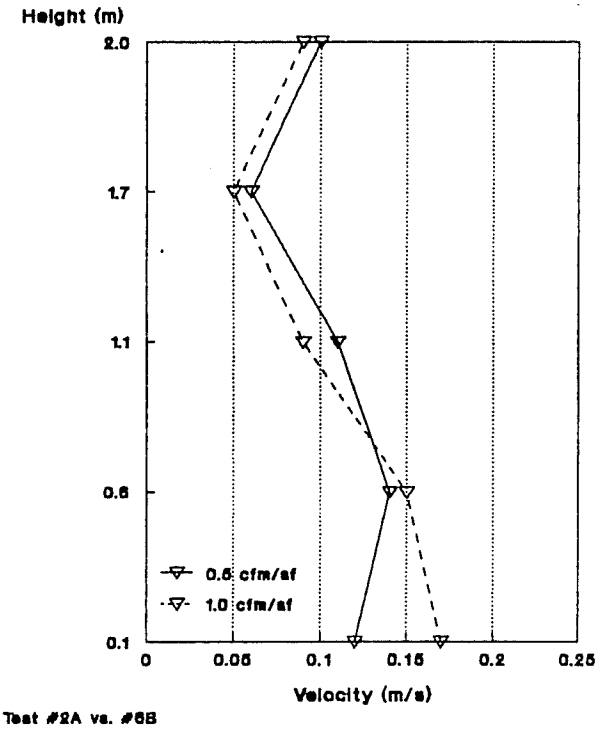

Test #2A vs. #6B

WS #1

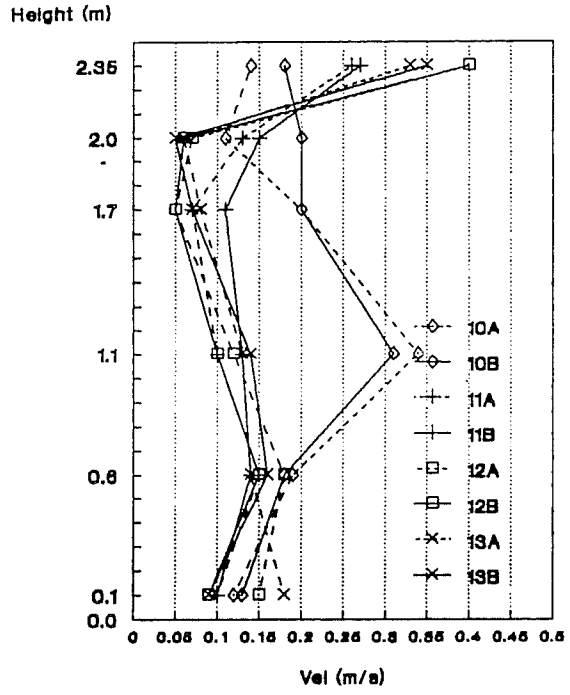

Figure 13. Diffuser location: Velocity effects

Tests: 10A&B, 11A&B
12A&B, 13A&B

WS #2

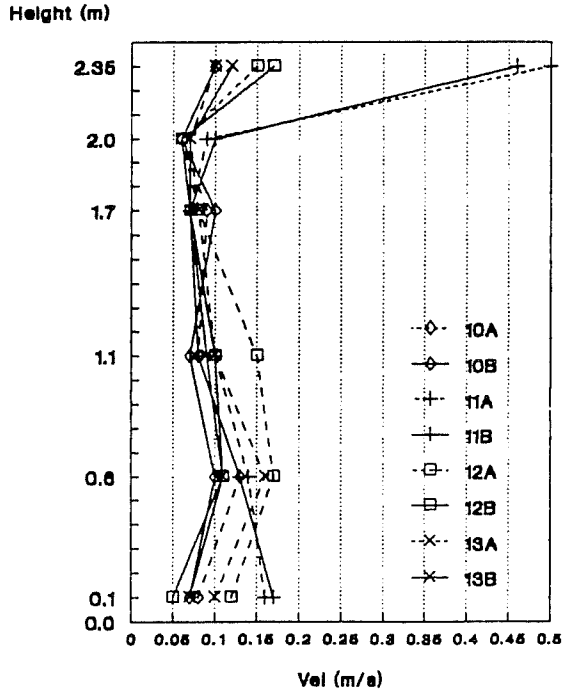

WS #3

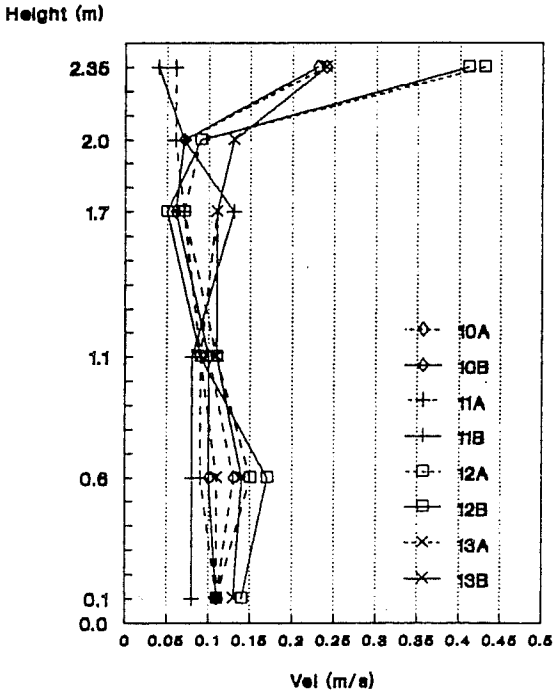

WS #1

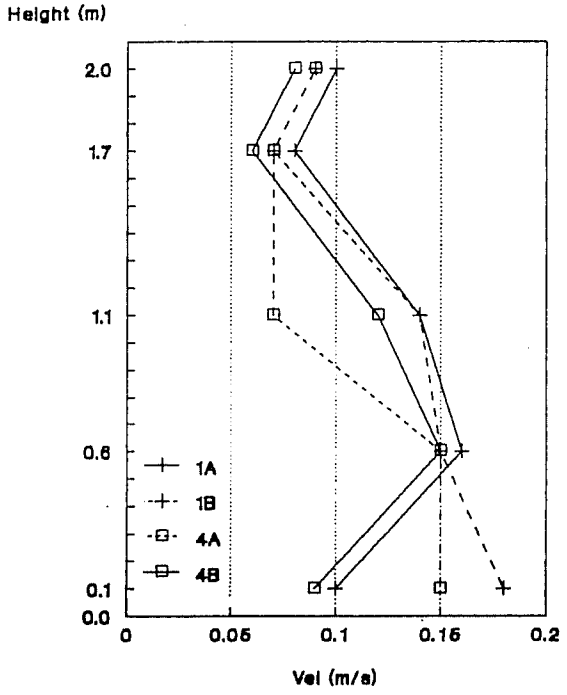

Figure 14A.

Heat load density: Velocity effects

Tests: 1A, 1B, 4A, 4B

WS #2

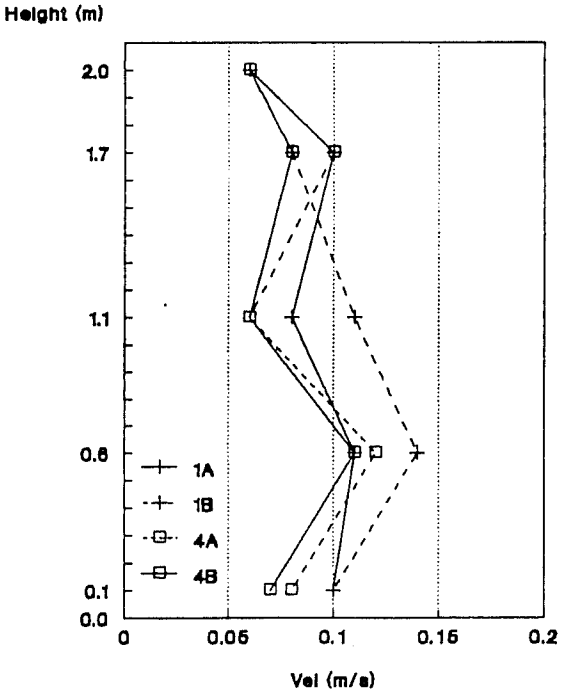

WS #3

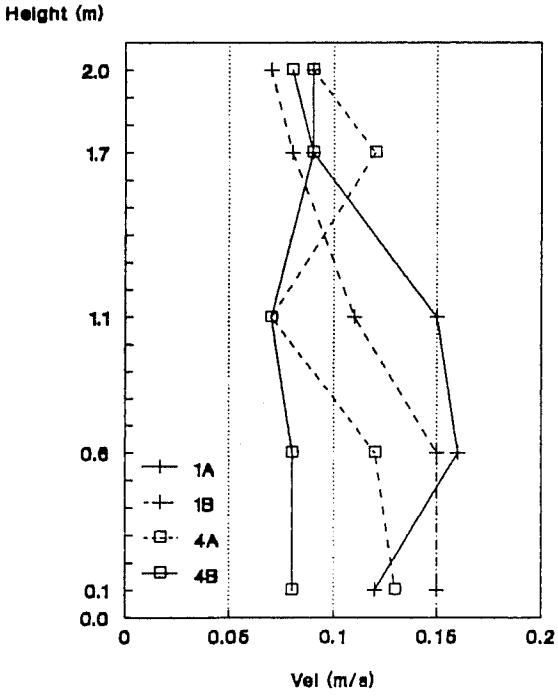

WS #1

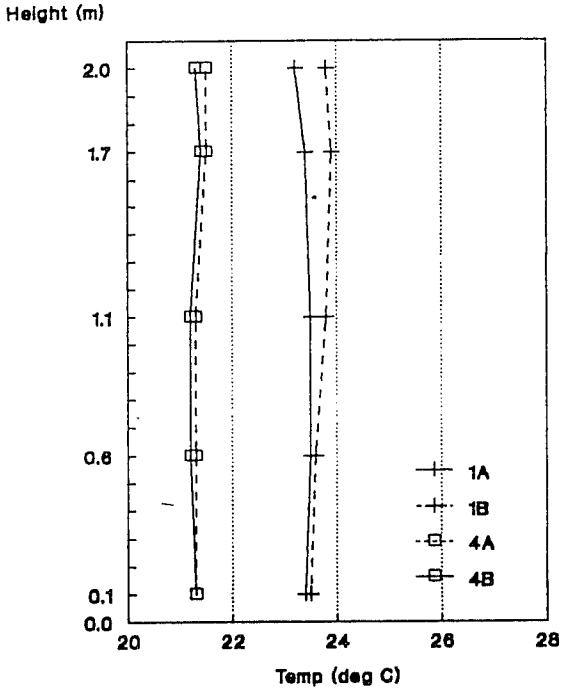

Figure 14B.
Heat load density: Temperature effects

Tests: 1A, 1B, 4A, 4B

WS #2

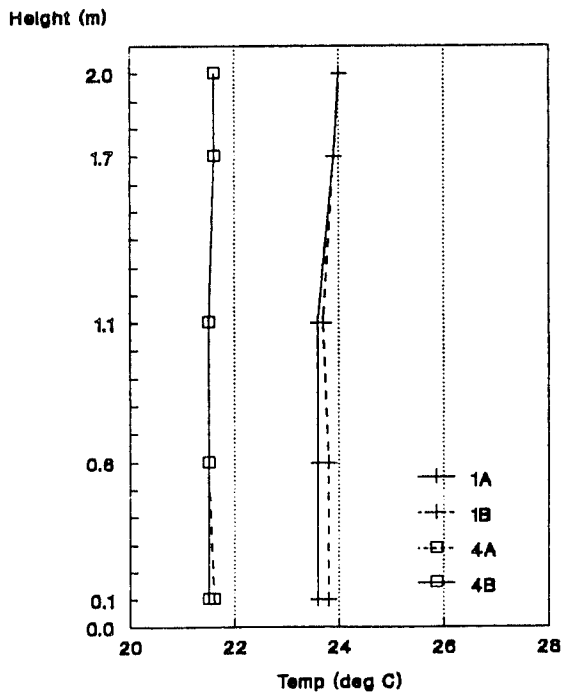

WS #3

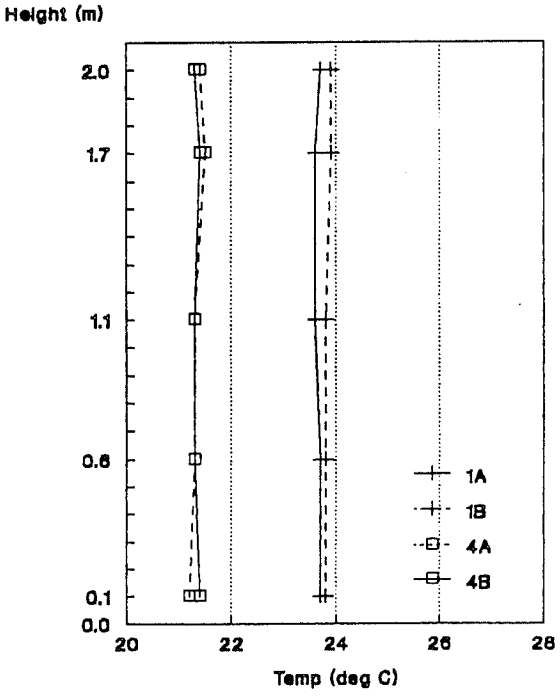

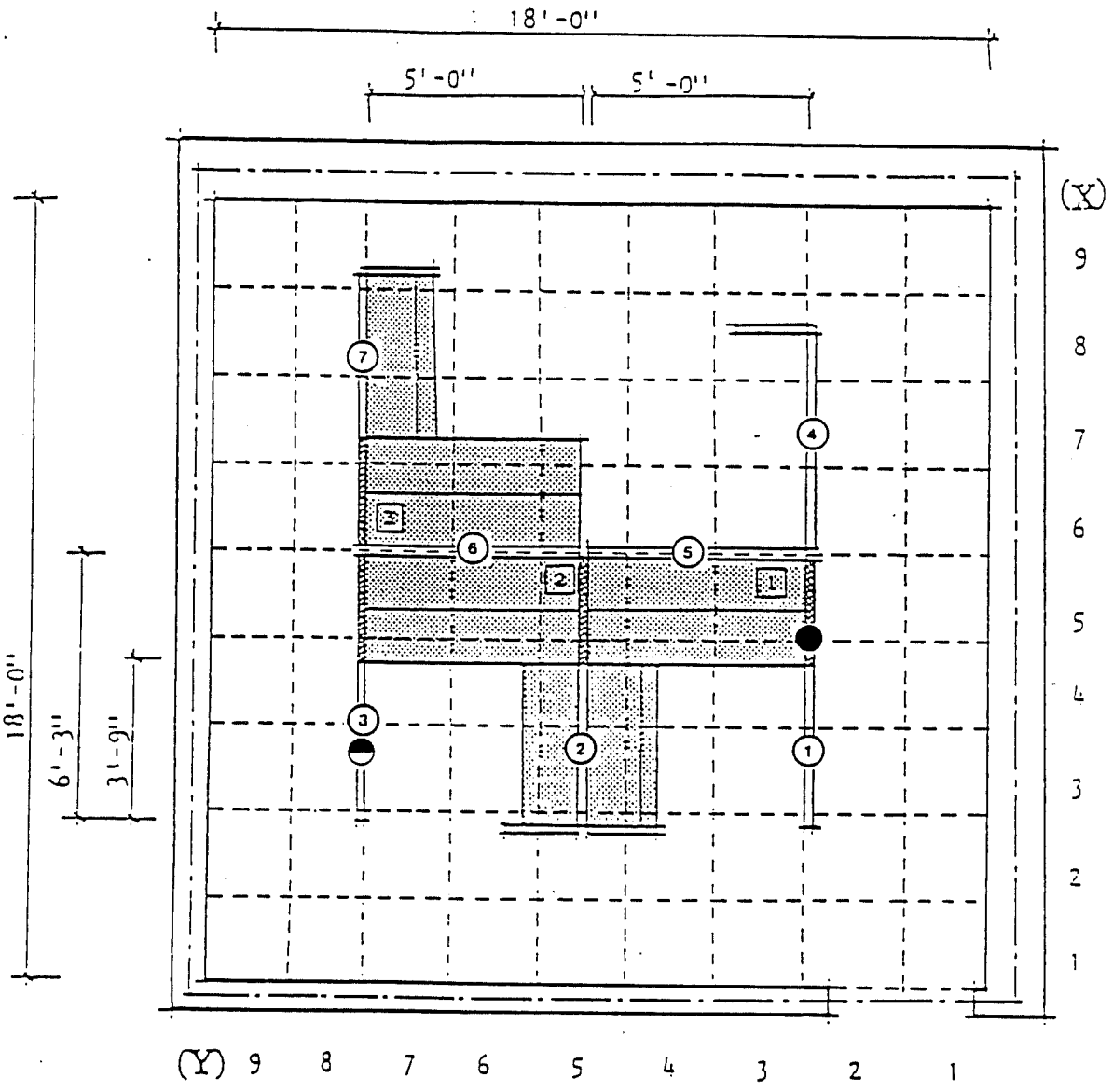

Figure 15. Air Gap Velocity Measurement Locations:Test 12A

● Solid Partition
◓ Airflow/Solid Partition

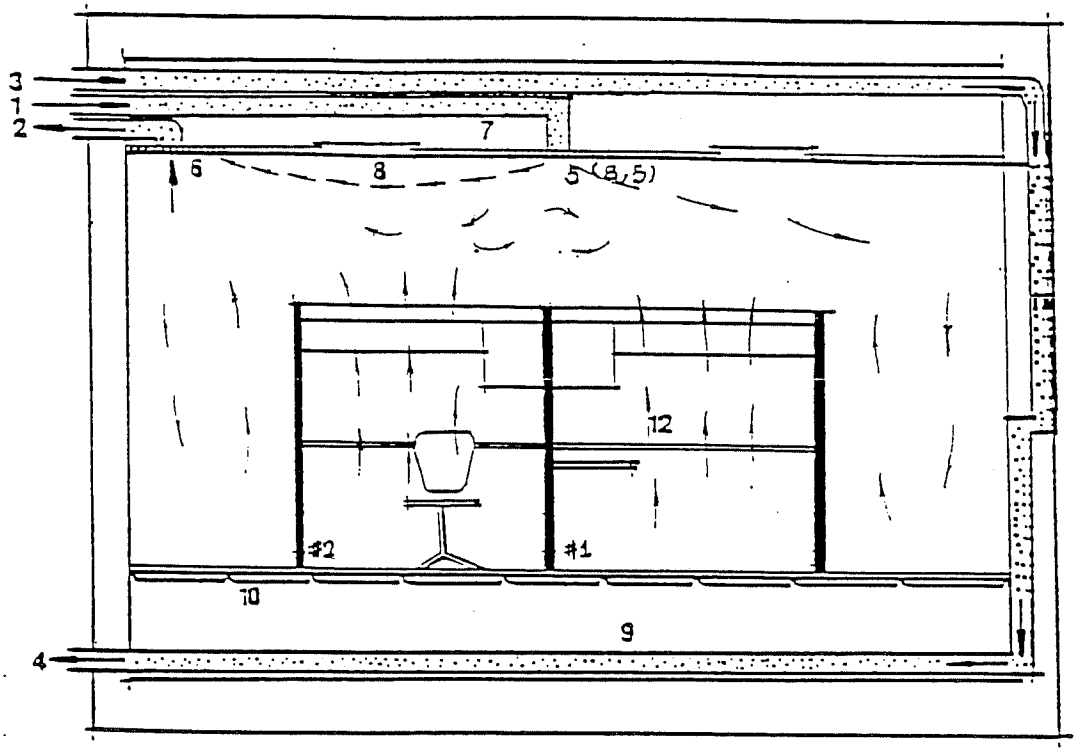

Figure 16a. Flow Visualization:
Test 10B with solid partitions

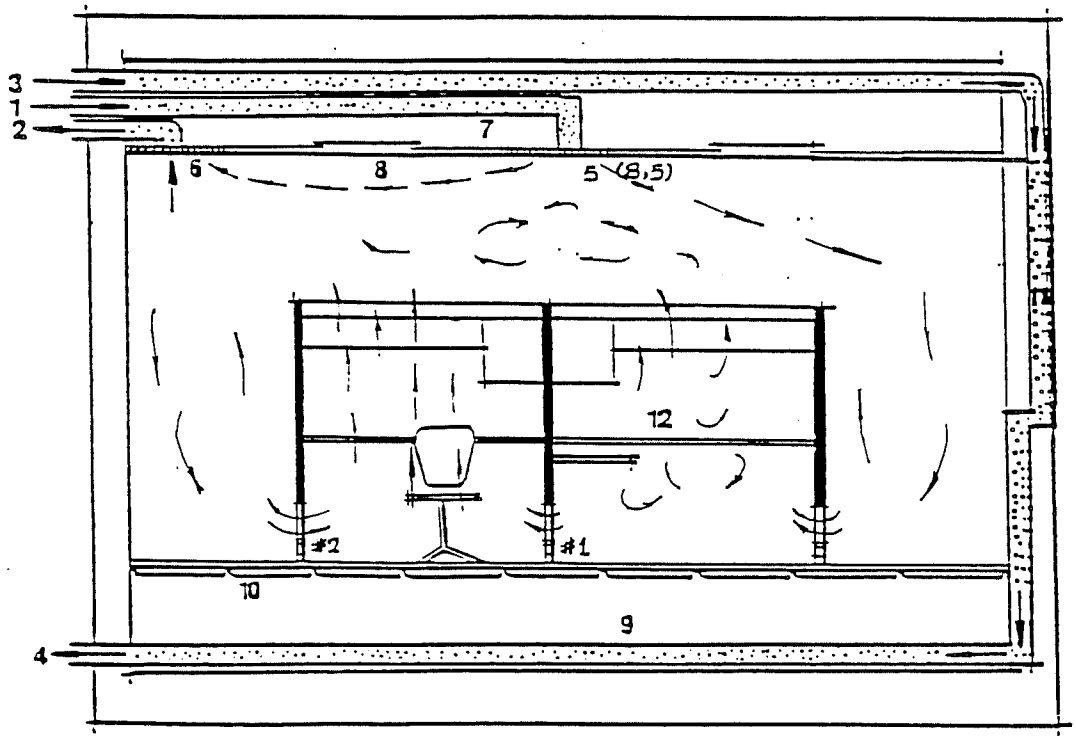

Figure 16b. Flow Visualization:
Test 10A with airflow partitions

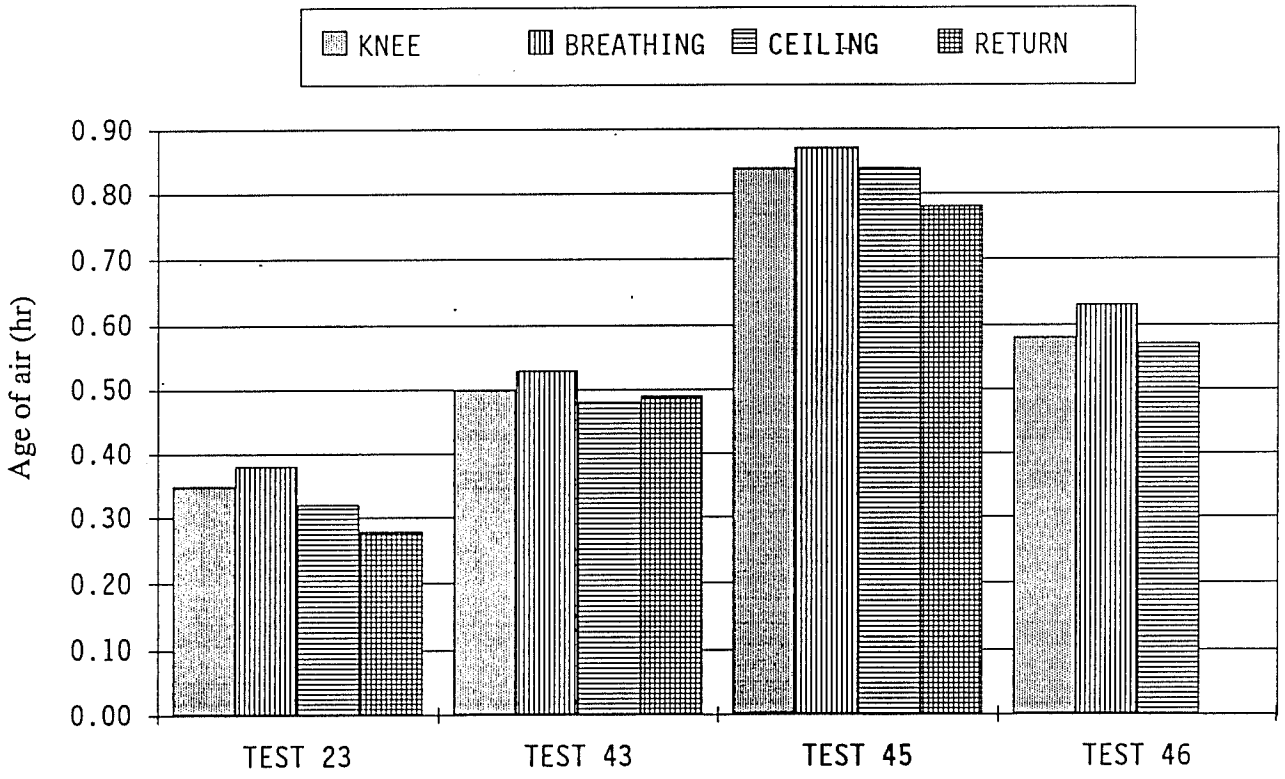

Figure 17. Variations in Age of Air with Height

Average age at the knee level for all workstations, average age at the breathing level for all workstations, average age near the ceiling level above all workstations, and the age in the return duct. Ages are grouped by heating tests.

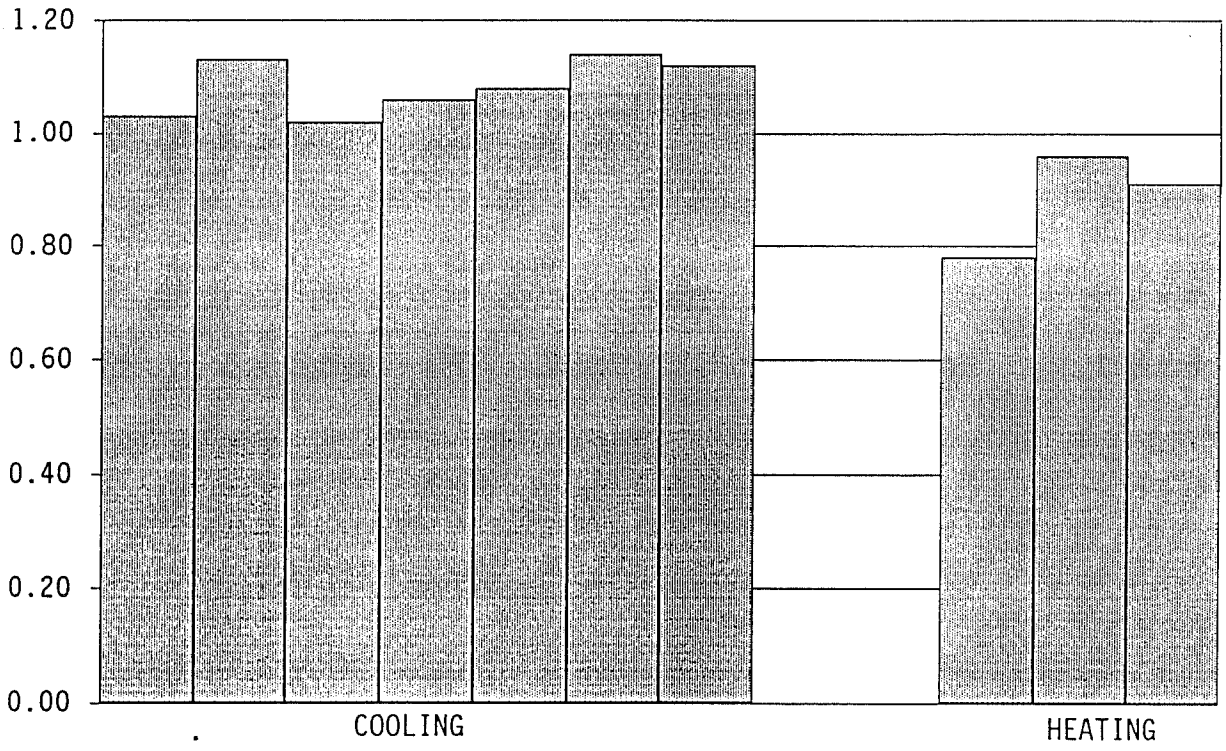

Figure 18. Short-Circuiting

Age of air in the return duct divided by the average age of air of all workstations at the breathing level and knee level. Ratios from heating tests and cooling tests are in separate groups. Tests with mixing fans operating are not included.